Comprehensive Automobile Research System (CARS) – a Python-based Automobile Emissions Inventory Model

3 Bok H. Baek[1], Rizzieri Pedruzzi[2], Minwoo Park[3], Chi-Tsan Wang[1], Younha Kim[4], Chul-Han
4 Song[5], and Jung-Hun Woo[3,6]

5 [1]Center for Spatial Information Science and Systems – George Mason University, Fairfax, VA, USA.

6 [2]Department of Sanitary and Environmental Engineering, Federal University of Minas Gerais, Belo Horizonte,
7 Brazil.

8 [3]Department of Technology Fusion Engineering, College of Engineering, Konkuk University, Seoul, Republic of
9 Korea

10 [4]Energy, Climate, and Environment program, International Institute for Applied Systems Analysis, Laxenburg,
11 Austria

12 [5]School of Earth and Environmental Engineering, Gwangju Institute Science and Technology, Gwangju, Republic of
13 Korea

14 [6]Civil and Environmental Engineering, College of Engineering, Konkuk University, Seoul, Republic of Korea

15 *corresponding to: Jung-Hun Woo* (jwoo@konkuk.ac.kr)

Abstract

The Comprehensive Automobile Research System (CARS) is an open-source python-based automobile emissions inventory model designed to efficiently estimate high quality emissions from motor-vehicle emission sources. It can estimate the criteria air pollutants, greenhouse gases, and air toxics in various temporal resolutions at the national, state, county, and any spatial resolution based on the spatiotemporal resolutions of input datasets. The CARS is designed to utilize the local vehicle activity data, such as vehicle travel distance, road link-level network Geographic Information System (GIS) information, and vehicle-specific average speed by road type, to generate a temporally and spatially resolved automobile emissions inventory for policymakers, stakeholders, and the air quality modeling community. The CARS model adopted the European Environment Agency's (EEA) onroad automobile emissions calculation methodologies to estimate the hot exhaust, cold start, and evaporative emissions from onroad automobile sources. It can optionally utilize average speed distribution (ASD) of all road types to reflect more realistic vehicle speed variations. Also, utilizing high-resolution road GIS data allows the CARS to estimate the road link-level emissions to improve the inventory's spatial resolution. When we compared the official 2015 national mobile emissions from Korea's Clean Air Policy

Support System (CAPSS) against the ones estimated by the CARS, there is a moderate increase of volatile organic compounds (VOCs) (33%), carbon monoxide (CO) (52%), and fine particulate matter ($PM_{2.5}$) (15%) emissions while nitrogen oxides (NOx) and sulfur oxides (Sox) are reduced by 24% and 17% in the CARS estimates. The main differences are driven by the usage of different vehicle activities and the incorporation of road-specific ASD, which plays a critical role in hot exhaust emission estimates but wasn't implemented in Korea's CAPSS mobile emissions inventory. While 52% of vehicles use gasoline fuel and 35% use diesel, gasoline vehicles only contribute 7.7% of total NOx emissions while diesel vehicles contribute 85.3%. But for VOC emissions, gasoline vehicles contribute 52.1% while diesel vehicles are limited to 23%. While diesel buses are only 0.3% of vehicles, each vehicle has the largest contribution to NO_x emissions (8.51% of NO_x total) due to it having longest daily vehicle kilometer travel (VKT). In VOC emission part, CNG buses are the largest contributor with 19.5% of total VOC emissions. For primary $PM_{2.5}$, more than 98.5% is from diesel vehicles. The CARS model's in-depth analysis feature can assist government policymakers and stakeholders develop the best emission abatement strategies.

Keywords: inventory: automobile, vehicle emissions, hot exhaust, cold start, evaporative, python

1 Introduction

Globally, ambient pollution causes more than 4.2 million premature deaths every year (Cohen et al., 2017), and Burnett et al. estimate the health burden is closer to 9 million deaths from ambient PM concentrations (Burneet et al, 2018). To effectively mitigate air pollutants, both developed and developing countries' governments have been implementing stringent air pollution abatement control policies to reduce harmful regional air pollutants (Hogrefe et al., 2001a; Hogrefe et al., 2001b; Dennis et al., 2010; Rao et al., 2011; Appel et al., 2013; Luo et al., 2019). The CTM simulation results strongly rely on precise input data, such as emission inventory, meteorology, land surface parameters, and chemical mechanisms in the atmosphere.

The transportation emission sector is one of the major anthropogenic emissions in urban areas. The tailpipe emissions from the vehicle's combustion process contain many air pollutants, including nitrogen oxides (NOx), volatile organic compounds (VOCs), carbon monoxide (CO), ammonia (NH_3), sulfur dioxide (SO_2), and primary particulate matter (PM) which will participate in the formation of detrimental secondary pollutants like ozone and $PM_{2.5}$ in the atmosphere. In the Seoul Metropolitan Area (SMA) in South Korea, transportation automobile sources contribute the most to the total NO_X and primary $PM_{2.5}$ emissions across all emission sources. (Choi et al., 2014; Kim et al., 2017a; Kim et al., 2017b; Kim et al., 2017c). Thus, it is critical to understand and represent better on the emission patterns from the transportation automobile sources in the CTM model. The use of process-based automobile emission models is highly recommended to meet the

68 needs in CTM model because it can estimate the highly resolved spatiotemporal automobile
69 emissions. (Moussiopoulos et al., 2009; Russell and Dennis, 2000).

70   There are two methodologies known in emission inventory development: top-down and
71 bottom-up. The choice of methods is determined by the input data availability. The top-down
72 approach primarily relies on the aggregated and generalized country or regional information,
73 especially in developing countries where only limited datasets and information are available. It has
74 its limitations on representing the vehicle emission process realistically due to the lack of detailed
75 activity and ancillary supporting data. However, the bottom-up approach requires higher-quality
76 spatiotemporal activity datasets like road network information, vehicle composition (vehicle type,
77 engine size, vehicle age, and fuel-technology), pollutant-specific emissions factors, road segment
78 length, traffic activity data, and fuel consumption (EEA, 2019; Ibarra-Espinosa et al., 2018b;
79 IEMA, 2017). It can generate more accurate and detailed automobile emissions across various
80 operating processes, such as hot exhaust, evaporative, idling, and hot soak (Nagpure et al., 2016;
81 Ibarra-Espinosa et al., 2018a).

82   There are several bottom-up mobile emissions models available, like MOVES (MOtor
83 Vehicle Emissions Simulator) from the U.S. Environmental Protection Agency (USEPA), the
84 European Environment Agency's (EEA) model COPERT (COmputer Programmed to calculate
85 Emissions from Road Transport), the HERMES (High-Elective Resolution Modelling Emission
86 System) from Barcelona Supercomputing Center (Guevara et al., 2019), the VEIN (Vehicular
87 Emissions INventory) model developed by Ibarra-Espinosa et al. (2017), and the VAPI (Vehicular
88 Air Pollution Inventory) model developed by Nagpure and Gurjar (2012) for India (Nagpure et al.,
89 2016). While these models are all bottom-up emission inventory models, a single model cannot
90 meet all modelers, policymakers, and stakeholders' needs because each model holds its own pros
91 and cons. They are developed differently to meet specific user needs based on the types of traffic
92 activity and emission factors, emission calculation methodologies, and other optional/available
93 traffic-related inputs such as average speed distribution and geographical resolution. Each model
94 is developed with different levels of specificity, underlying data set and modeling assumptions.

95   The MOVES model has the strength to generate high-quality emissions for up to 16
96 different emission processes (i.e., Running Exhaust, Start Exhaust, Evaporative, Refueling,
97 Extended Idling, Brake, Tire, etc.). It can simulate not only county-level but also road segment
98 level depending on data availability. It can also reflect local meteorological conditions, such as
99 ambient temperature and relative humidity, which can significantly impact both pollutants and
100 emissions processes (Choi et al., 2017; Perugu et al., 2018). Disadvantage of this model is it
101 difficult to update and apply to countries outside of the U.S. because MOVES model has a high
102 degree of specificity. The COPERT model that is widely used in European countries has its
103 advantages, such as the capability to model emissions in high resolution. Additionally, it is fully
104 integrated with the EEA's onroad vehicle emissions factors guidelines and can generate a complete
105 quality assurance (QA) and visualization summary (Ntziachristos et al., 2009). The cons are that

it is a proprietary commercial licensed software, limited to EEA guidance, and challenging to modify and update with any key input datasets like the latest emission factors from non-European countries (Lejri et al., 2018; Rey DR, 2021; Li et al., 2019; Lv et al., 2019; Smit et al., 2019).

The HERMES and VEIN are both recently released bottom-up inventory models. They have their pros in that they are both open-source models based on open-source computing languages (Python and R), which provide transparency of emission calculations with a considerable amount of data behind it (Ibarra-Espinosa et al., 2018b; Guevara et al., 2019). Both models are driven by comma-separated value (CSV) formatted input files, making it very easy for users to modify the input datasets. They are also based on the EEA's emission calculation method and equipped with a complete QA and visualization tool based on Python and R libraries. However, it is not an easy task to update the emission factors, and generate other required input datasets for other countries, and lacks support for any control strategy plan feature to generate a responsive reduced emissions inventory for policymakers, stakeholders, and modelers.

The VAPI (Vehicular Air Pollution Inventory) model was developed in India because the country does not have an extensive and robust traffic-related dataset to run these kinds of vehicular emissions inventory models (Nagpure et al., 2016; Perugu, 2019).

There are also a few shortcomings of incorporating these bottom-up models into CTM studies. These models require strong programming skills to operate, such as collecting and preparing the input data to fit the model requirement, configuring the model variables, and changing specific variables that may be embedded in the code. Another downside is that while the administration-level emissions inventory can be estimated by those models, it requires a 3rd party emissions processor like the SMOKE (Sparse Matrix Operator Kerner Emissions) modeling system (Baek and Seppanen, 2021) to process and generate spatially and temporally resolved emissions inputs for CTM. Some detailed information, like link-level hourly driving patterns, can be lost in the emissions processing steps.

There is no single model capable of meeting all the requirements across various spatial and temporal scales (Pinto et al., 2020). However, transparency, simplicity, and a user-friendly interface are requirements for those who mainly work in transportation policy and air quality modeling development (Fallahshorshani et al., 2012; Kaewunruen et al., 2016; Sallis et al., 2016; Sun et al., 2016; Tominaga and Stathopoulos, 2016). Thus, the ideal mobile emissions modeling system would be computationally optimized, easy-to-use, and have a user-friendly interface. Additionally, the model should easily adapt detailed local activity information and the state-of-art emission factors as an input to represent them in the highest resolution possible in time and space.

We have developed the Comprehensive Automobile Research System (CARS) to meet these requirements, especially for the air quality research community, policymakers, and air quality modelers. The CARS is a stand-alone, fully modularized, computationally optimized, python-based automobile emission model. The modularization improves the efficiency of processing times.

143 Once district and road link-level annual/monthly/daily total emissions are computed, the rest of
144 the processes are optional. It can generate chemically speciated, spatially gridded hourly emissions
145 for CTMs without any 3rd party emissions modeling system to develop the highest quality CTM-
146 ready emissions inputs. All functions are operated by independent modules and can be enabled by
147 users. Details on modularization will be discussed later. The CARS model can be easily adopted
148 and is simple for users to add new functions or modules in the future. The application of the CARS
149 to South Korea will be described in detail later.

2   CARS Emissions Calculation

151   The CARS is an open-source Python-based customizable motor vehicle emissions
152 processor that estimates onroad and offroad emissions for specific criteria and toxic air pollutants.
153 Figure 1 is a schematic of the CARS overview. It applies vehicle, engine, and fuel specific
154 emission factors to traffic data to estimate the local level annual, monthly, and daily total emissions
155 inventory. The emissions inventory calculations require the list of pollutant-specific emissions
156 factors by vehicle age, local activity data, average speed profile/distribution by road type, and
157 geographic information system (GIS) road segment shapefiles inputs. The spatial resolution of
158 vehicle kilometer travel (VKT) defines the CARS geographic scale (i.e. district, county, state, and
159 country) for emission calculations. Unlike the district-level Korea Clean Air Policy Support
160 System (CAPSS) automobile emission inventory (Lee et al., 2011a; Lee et al., 2011b), the CARS
161 applies high-resolution annual average daily traffic (AADT) data from the road GIS shapefiles to
162 distribute the total district emissions into road link-level emissions. Optionally, these road link-
163 level emissions can be used to generate spatially gridded CTM-ready emissions input data once
164 the output modeling domain is defined. The summary of input files by categories are presented in
165 Appendix H. How the CARS estimates spatially and temporally enhanced automobile emissions
166 inventories will be discussed in detail next chapter.

167   South Korean traffic databases from the Korea CAPSS team (Lee et al., 2011b) from the
168 National Institute of Environmental Research (NIER) were used in this study to compute the
169 updated onroad automobile emissions inventory. The databases include individual vehicle activity
170 data (daily total VKT), road activity data (average speed distribution by road), vehicle age specific
171 emission factors, road type information, surface weather data, and GIS road shapefiles.

2.1   Individual Daily Average VKT Activity Data

173   The individual vehicle VKT data is used to reflect the human activity. This study imported
174 the national registered vehicle-specific daily total VKT from South Korea's Vehicle Inspection
175 Management System (VIMS), which belongs to the Korea Transportation Safety Authority
176 (KTSA). It contains over 50 million records from 2013 to 2017. For the CARS model, we first
177 sorted these records by the vehicle identification number (VIN) to remove any duplicates and then

178   built vehicle-specific daily total VKT traffic activity data in the CSV format. The summary of
179   those vehicle numbers and VKTs is presented in Fig. 2. Sedan vehicles using gasoline fuel
180   comprise the greatest percentage of total vehicles at 47% (~10.4 million) and have the highest
181   VKT. Most vehicles demonstrate similar patterns between the number of vehicles and daily VKT.
182   However, as expected, LPG (liquefied petroleum gas)-fueled taxi are high in VKT compared to
183   the number of vehicles due to their daily long distance travel pattern.

184   The VIN (*vin*) information is used to calculate vehicle-specific daily average VKT (VKT_{vin},
185   km d^{-1}). In Eq. (1), the individual daily average vehicle VKT (VKT_{vin}) is calculated based on the
186   cumulative mileage ($M_{f;vin}$) between the last inspection date ($D_{f;vin}$) and registration date ($D_{0;vin}$).
187   Each vehicle is categorized with Korea's NIER which defines the vehicle types (Ryu et al., 2003;
188   Ryu et al., 2004; Ryu et al., 2005; Lee et al., 2011a) based on a combination of vehicle types (e.g.,
189   sedan, truck, bus, etc), engine sizes (e.g., compact, full size, midsize, etc) and fuel types (e.g.,
190   gasoline, diesel, LPG, etc). Full details of vehicle types and daily total VKT are shown in Appendix
191   A and B.

192
$$VKT_{vin} = \frac{M_{f;vin}}{D_{f;vin} - D_{0;vin}} \qquad (1)$$

193   **2.2   Emission Calculations**

194   Automobile emission sources include motorized engine sources on the paved road network
195   and off the road network (e.g., drive way and parking lots). The CARS model doesn't simulate
196   emissions from nonroad emission sources, such as aviation, railways, construction, agricultures,
197   lawn mower, and boats yet. The CARS model simulates the onroad automobile emissions from
198   network roads using their local traffic-related datasets. The following section explains the
199   approach of the onroad automobile emission processes. The onroad emission (E_{onroad}) in the CARS
200   is defined in Eq. (2), which includes three major emission processes (Ntziachristos and Samaras,
201   2000):

202
$$E_{onroad} = E_{hot} + E_{cold} + E_{vap} \qquad (2)$$

203   The hot exhaust emissions (E_{hot}) are the vehicle's tailpipe emissions when the internal combustion
204   engine (ICE) combusts the fuel to generate energy under the average operating temperature. The
205   cold start emissions (E_{cold}) are the tailpipe emissions from the ICE when the cold vehicle engine is
206   ignited and the operational temperature is below average condition. The evaporative VOC
207   emissions (E_{vap}) are the emissions evaporated/permeated from the fuel systems (fuel tanks,
208   injection systems, and fuel lines) of vehicles.

209   The CARS first applies the hot exhaust emission factors by vehicle type, age, fuel, engine,
210   and pollutants to individual daily total VKT to compute the hot exhaust emissions. The rest of the

211 processes for cold start and evaporative emissions are calculated afterwards. The emission
212 calculation methodologies used in the CARS model are based on tier 2 and tier 3 methodologies
213 from the EEA's mobile emission inventory guidebook (EEA, 2019) to be consistent with Korea's
214 National Emission Inventory System (NEIS) (Lee et al., 2011a).

2.2.1 Hot Exhaust Emissions

216 Hot exhaust emissions, which is from the vehicle's tailpipe, is the exhaust gas from the
217 combustion process in an ICE. The ICE combustion cycle generally causes incomplete combustion
218 processes which emit hydrocarbons, carbon monoxide (CO), and particulate matter (PM) which
219 not completely controlled from the aftertreatment equipment, such as three-way catalytic converter
220 and released into the atmosphere. The sulfur compounds in the fuel are oxidized and become sulfur
221 oxides (SO_x). Nitrogen oxides (NO_x) are produced due to the abundance of nitrogen (N_2) and
222 oxygen (O_2) during the combustion process.

223 Equation 3 represents the calculation of daily individual vehicle hot exhaust emission rate,
224 $E_{hot; p,vin,myr}$ (g d^{-1}) of pollutant (p). An individual vehicle-specific daily VKT_{vin} (km d^{-1}) is estimated
225 by Eq. (1). The $EF_{hot;p,v,myr,s}$ (g/km) is the hot exhaust emission factor of pollutants (p) for the
226 vehicle type (v), vehicle manufacture year (myr), and average vehicle speed (s). The district's total
227 emission rate is the total hot exhaust emissions from all individual vehicles within the same district.

228
$$E_{hot; p,vin,myr} = DF_{p,v,myr} \times VKT_{vin} \times EF_{hot; p,v,myr,s} \qquad (3)$$

229 The deterioration factor (DF) in Eq. (3) is an optional function in the CARS. The
230 deterioration process is caused by vehicle aging and can lead to the increase of vehicle emissions.
231 The vehicle DF is varied by vehicle type (v), pollutant (p), and vehicle manufacture year (myr).
232 The CARS model computes vehicle ages based on the vehicle manufacture year and model
233 simulation year. According to the guidance of deterioration factors calculation from NIER, there
234 is no deterioration in a new vehicle during their first five years. After five years, the deterioration
235 factors can increase the 5~10% range depending on the type of vehicle and pollutants.
236 Deterioration processes can cause up to 100% increase of emissions in fifteen-year-old vehicles.
237 Currently, the DF is an empirical coefficient that varies by vehicle age (Lee et al., 2011a).

238 The hot exhaust emission factor, $EF_{hot;p,v,s}$ (g/km) is a function of vehicle speed (s) with
239 other empirical coefficients: a, b, c, d, f, k. The emission factor formula and those coefficients
240 were developed by NIER CAPSS (Lee et al., 2011a). These coefficients are varied by pollutants
241 (p), vehicle type (v), vehicle manufacture year (myr), and vehicle speed (s). The vehicle speed
242 affects the combustion efficiency of an ICE and impacts the emission rates and its composition
243 from the tailpipe.

244
$$EF_{hot; p,v,myr,s} = k(a \times s^b + c \times s^d + f) \qquad (4)$$

245   While vehicle speed plays a critical role in hot exhaust emissions from most vehicles, NOx

246 emissions from some diesel vehicles show sensitivity to local ambient temperature along with

247 vehicle speed (Ntziachristos and Samaras, 2000). Figure 3 shows the dependency of NO_x emission

248 factors from compact diesel vehicles to vehicle speed (Fig. 3a) and ambient temperature (Fig. 3b).

249 Figure 3a shows a significant decrease of NO_x emissions while speed increases between 0 and 70

250 km. Figure 3b demonstrates the significance of local meteorology on NO_x emissions from a

251 compact diesel sedan. Based on these NIER's CAPSS emission factors, the sensitivity to local

252 ambient temperature is limited to NO_x pollutant emissions from diesel vehicles.

253   Due to its high sensitivity to the vehicle operating speed, it is important for the CARS to

254 simulate realistic speed patterns for accurate emissions estimates. When a single speed is assigned

255 to compute hot exhaust emissions, it won't reflect the emissions under low-speed circumstances.

256 To overcome this limitation, the CARS has adopted the 16 average speed bins concepts for a better

257 representation of vehicle speed distribution that varies by road type (i.e., local, highway,

258 expressway). We have implemented a feature for the CARS optionally to apply road-specific

259 average speed distributions (ASD) ($A_{bin,r}$), which represents the fractions of 16-speed bins (*bin*)

260 (from 0 to 121 km h^{-1} defined in Appendix E) for eight different road types (*r*) (No.101-108, shown

261 in Appendix C) as classified by CAPSS (Fig. 4a). Although ASD patterns vary by region and time,

262 current CARS model version does not support ASD application by region and time of day due to

263 the lack of region and time-dependent ASD availability in South Korea.

264   We first developed the ASD (Fig. 4a) for eight different road types (No. 101-108) in South

265 Korea based on the latest road link-specific average speed and the length of link from the SK GIS

266 road network shapefiles (NIER, 2018). However, the ASD based on the SK GIS road shapefiles

267 did not capture low-speed range (<16 km h^{-1}) driving (Fig. 4a). This causes a significantly lower

268 estimation of NOx and VOC emissions compared to the CAPSS (Appendix G). We believe the

269 SK average speed distribution is missing low-speed driving that can occur on links on different

270 days due to traffic congestion. To address this absence of low-speed driving in the SK ASD, we

271 incorporated data from the ASD (Figure 4b) from the state of Georgia developed by U.S. EPA to

272 the low-speed ranges (speed bin #1 and #2 for road type 1 to 7). We increased the total fractions

273 of low-speed bins (the 2:1 ratio of fractions of bin #1 and #2) by 2% for interstate expressways,

274 3% for urban expressways, 7% for all highways, and 15% for all local roads. The increases in low-

275 speed bins lowered the distributions of other higher speed bins homogeneously due to the

276 renormalization of fractions by road type. Figure 4c shows the renormalized hybrid-ASDs of all

277 road types based on SK ASD and Georgia ASD. We understand, the hybrid-ASD approach is not

278 ideal for SK onroad emission inventory development. However, it clearly demonstrates the

279 CARS's capability and sensitivity to the vehicle speed representation and the impacts of ASD to

280 the local onroad mobile inventories.

281   While 16-speed bins ASD application is critical to computing more realistic hot exhaust

282 emissions, there should be some restrictions on certain road types. Users can adjust the restricted

283 roads control table input file to limit the vehicle types that can only be operated on a particular
284 road type. For example, motorcycles are limited to local roads (No. 104, 106, and 107), but not on
285 expressways (No. 101, 102, 103, 105, and 108) due to its traffic regulation rules. Heavy trucks are
286 only allowed on the highway (No. 101, 102, 103, 105, and 108.) by law. The details of the road
287 restriction control table format can be found on the CARS's user's guide from the CARS Github
288 website (https://github.com/bokhaeng/CARS/tree/master/docs/User_Manual).

289 The 16-speed bins averaged speed distribution calculated by road type ($A_{bin,r}$) and road type
290 weight factors ($\omega_{r,d}$) in a district (d) from Eq. (13) are added to the CARS hot exhaust emissions
291 equation (Eq. 3). The hot exhaust emissions from individual vehicles ($E_{hot;p,vin,myr}$) can be
292 calculated by considering road-specific speed bins distribution (Eq. 5). Although the vehicles may
293 be operated in different districts from their registered district, this is our best method to estimate
294 the vehicle speed for hot exhaust emissions.

295
$$E_{hot;\,p,vin,myr} = DF_{p,v,myr} \times \sum_{bin}(VKT_{vin} \times EF_{hot;\,p,v,myr,s} \times A_{bin,r}) \qquad (5)$$

296 **2.2.2 Cold Start Emissions**

297 The cold start emissions occur when a cold-engine vehicle is ignited. The lower
298 temperature of the ICE is not an optimal condition for complete fuel combustion. This process
299 lowers the combustion efficiency (CE) and increases the emissions of hydrocarbon and CO
300 pollutants from the tailpipe exhaust (Jang et al., 2007). The CARS can estimate the cold start
301 emissions for vehicles using gasoline, diesel, or liquefied petroleum gas (LPG) fuel. Besides the
302 vehicle and engine type, road type also plays a critical role in the quantity of cold start emissions
303 because it occurs mostly in parking lots and rarely on highways.

304 The cold start emission, E_{cold} (g d^{-1}), is derived from the hot exhaust emissions, the ratio of
305 hot to cold exhaust emissions (EF_{cold}/EF_{hot} -1.0), and the percentage of the traveled distance with
306 a cold engine (Eq. 6).

307
$$E_{cold;\,p,v} = \beta_T \times E_{hot;\,p,v} \times \left(\frac{EF_{cold;\,p,v}}{EF_{hot;\,p,v}} - 1.0\right) \qquad (6)$$

308 The emission factor of cold start emissions (EF_{cold}) is not directly calculated from
309 measurement data like hot exhaust emissions ($E_{hot;p,v}$), but measured under different ambient
310 temperatures (T). The CARS model applies linear regression models developed by CAPSS to
311 estimate the increasing ratio of cold start to hot exhaust emissions (EF_{cold}/EF_{hot}) under different
312 temperatures (T) (Eq. 7). In this equation, A and B are the empirical coefficients that vary by the
313 pollutants (p) and vehicle type (v).

314
$$\left(\frac{EF_{cold;\,p,v}}{EF_{hot;\,p,v}}\right) = A_{p,v} + B_{p,v} \times T \qquad (7)$$

315   β is the percentage of the distance traveled under a cold engine. It also depends on the
316 ambient temperature. Cold ambient temperatures cause a longer distance traveled under a cold
317 engine due to the slower heating time. According to the CAPSS database for Seoul city (Lee et al.,
318 2011a), the empirical linear equation for β is shown in Eq. (8). This formula represents how
319 ambient temperature affects β. For example, when the average temperature is -2°C, β is 34.8%.
320 In summer, the monthly average temperature is 25.7°C, which causes β to drop to 21%.

321       $$\beta = 0.647 - 0.025 \times 12.35 - (0.00974 - 0.000385 \times 12.35) \times T \qquad (8)$$

322 **2.2.3   Evaporative VOC Emissions**

323   Evaporative emissions are emissions from vehicle fuel that are evaporated into the
324 atmosphere. This occurs in the fueling system inside the vehicle, such as fuel-tanks, injection
325 systems, and fuel lines. Diesel vehicles, however, can be exempted due to diesel fuel's low vapor
326 pressure. The primary sources of evaporative emissions are breathing losses through tank vents
327 and fuel permeation/leakage. The CARS model adopted the EEA's emission inventory guidebook
328 (EEA, 2019) to account for three mechanisms to estimate the evaporative VOC emissions (E_{vap}):
329 diurnal emissions from the tank (e_d), hot and warm soak emissions by fuel injection type (S_{fi}), and
330 running loss emissions (R) (Eq. 9). Unlike CAPSS, there is a conversion factor (0.075) applied to
331 E_{vap} for motorcycles to prevent an over-estimation of VOC.

332       $$E_{vap;\, p,v} = \left(e_{d;\, p,v} + S_{fi;\, p,v} + R_{l;\, p,v}\right) \qquad (9)$$

333   Diurnal emissions, e_d (g d^{-1}), during the daytime are caused by the ambient temperature
334 increase and the expansion of fuel vapors inside the fuel tank. Most of the current fuel tank systems
335 have emission control systems to limit this kind of evaporative VOC emissions. The e_d can be
336 calculated with the empirical Eq. (10), which was developed by CAPSS. T_l is the monthly average
337 of the daily lowest temperatures and T_h is the monthly average of the daily highest temperatures.
338 The empirical coefficient α is 0.2, which represents how 80% of emissions are eliminated by the
339 vehicle emission control system.

340       $$e_d = \alpha \times 9.1 exp[0.3286 + 0.0574 \times (T_l) + 0.0614 \times (T_h - T_l - 11.7)] \quad (10)$$

341   Soak emissions (S_{fi}) occur when a hot ICE is turned off; the remaining heat from the ICE
342 can increase the fuel temperature in the system. The carburetor float bowls are the major source of
343 the soak emissions. Newer vehicles with fuel injection and return-less fuel systems do not emit
344 soak emissions. Because most of the current vehicles in South Korea have a new fuel system, soak
345 emissions (S_{fi}) in the CARS model are set to 0.

346   The running loss emissions (R_l) are from vapors generated in the fuel tank when a vehicle
347 is in operation (Eq. 11). In some older vehicles, the carburetor and engine operation can increase

348 the temperature in the fuel tank and carburetor, which can cause a significant increase in
349 evaporative VOC emissions. VOC emissions from running loss can be greatly increased during
350 warmer weather. However, newer vehicles with fuel injection and return-less fuel systems are not
351 affected by the ambient temperature. Because most vehicles in South Korea do not use carburetor
352 technology, we expect running loss emissions to have the least impact (Lee et al., 2011b).

$$R_l = \alpha \times L_{r,v} \times [(1 - \beta) \times R_h + \beta \times R_w] \qquad (11)$$

354 The empirical coefficient α is 0.1 here, which represents that 90% of the running loss is
355 avoided by the newer fuel system. L is the distance traveled (km) by road and is the same one used
356 in hot exhaust emission calculations. β is the same parameter from Eq. (8). The R_h and R_w are the
357 average emission factors from running loss under hot and warm/cold conditions, respectively.

2.3 Road Link-Level Emissions Calculations

359 In general, district-level automobile emissions calculations are driven by district-level
360 averaged vehicle activity and operating data, which do not reflect realistic spatial patterns of
361 onroad automobile emissions. The CARS model introduces road link-specific traffic data by
362 default to develop spatially enhanced road link-specific emissions that reflect more representative
363 emissions by road link. This high-resolution traffic data is a GIS shapefile that is composed of
364 many connected segments, which are called "road links." All road links hold information such as
365 start/end location coordinates, AADT, road link length, averaged vehicle speed, and road type (No.
366 101-108).

367 The CARS model applies link-level AADT ($AADT_{d,r,l}$, d^{-1}) and road length ($L_{d,r,l}$) to
368 compute the road link-specific VKT ($VKT_{d,r,l}$, km d^{-1}) in Eq. (12). The road links are identified by
369 district (d), road type (r), and link (l) labels. The road VKT is a parameter that reflects the traffic
370 activity of each road link and it is different from individual daily vehicle activity data ($VKT_{v,age}$)
371 in Eq. (1).

$$VKT_{d,r,l} = AADT_{d,r,l} \times L_{d,r,l} \qquad (12)$$

373 Road link-specific VKT ($VKT_{d,r,l}$) is used to redistribute the district total emissions (E$_{onroad}$)
374 from Eq. 2 into road link-level emissions. The following three weight factors are computed: the
375 district weight factors, ω_d (Eq. 13), the road type weight factors, $\omega_{d,r}$ (Eq. 14), and the road-link
376 weight factors, $\omega_{d,l}$ (Eq. 15). The weight district factors (ω_d) are the renormalization of each
377 district's total VKT over state-level total VKT (N is the number of districts). The main reason we
378 performed the renormalization over state-level total VKT is to reflect daily traffic patterns from
379 multiple districts under the assumption that most vehicles travel within the same state. The road
380 type weight factors by district ($\omega_{r,d}$) are used to compute road-specific emissions, while road-

381 specific averaged speed distributions (ASD; $A_{s,r}$) from Eq. (5) are applied to capture vehicle
382 operating speeds by road type. The road link weight factors ($\omega_{d,l}$) are then applied to redistribute
383 the district emissions into road link-level emissions.

384

$$\omega_d = \frac{\sum_r \sum_l VKT_{d,r,l}}{\frac{1}{N} \sum_d \sum_r \sum_l VKT_{d,r,l}} \qquad (13)$$

$$\omega_{d,r} = \frac{\sum_l VKT_{d,r,l}}{\sum_r \sum_l VKT_{d,r,l}} \qquad (14)$$

$$\omega_{d,l} = \frac{VKT_{d,r,l}}{\sum_r \sum_l VKT_{d,r,l}} \qquad (15)$$

3   CARS Configuration

389   The CARS model is an open-source program based on Python (Guido van Rossum, 2009)
390 that allows the users to efficiently apply open-source modules to develop programs. Users can
391 easily install Python development tools and load customized packages and modules to set up the
392 CARS development environment. All CARS modules are developed using Python v3.6. Other than
393 the GIS road shapefiles, all input files are based in the ASCII CSV format, which can be easily
394 handled by both spreadsheet programs and programming languages, making it more accessible for
395 users of all skillsets. The CARS can not only estimate district-level and spatially enhanced road
396 link-level emissions, but can also generate hourly chemically speciated gridded emissions for
397 CTMs. In addition, the CARS also generates various summary reports, graphics, and
398 georeferenced plots for quality assurance.

399   The required Python modules for the CARS are: "***geopandas,***" "***shapely.geometry***", and
400 "***csv***" modules to read the shapefiles and table data files. The "***NumPy***" and "***pandas***" modules
401 are used to operate the memory arrays and scientific calculations while the "***pyproj***" module deals
402 with converting the projection coordinate systems. "***matplotlib***" is for generating any type of
403 figures/plots. Furthermore, the CARS model can also read and write Climate and Forecast (CF)-
404 compliant NetCDF-formatted files using "***NetCDF4***".

405   The first process in the CARS is "***Loading_function_path***"; it allows users to define and
406 check the input file paths. Once all input files are checked, there are six process modules in CARS
407 to process inputs, compute emissions, and generate various output files, including QA reports.
408 Figure 5 is the schematic of the CARS that consists of six process modules with various functions.
409 The six process modules are (1) "**Process activity data**", (2) "**Process emission factors**", (3)
410 "**Process shapefile**, (4) "**Calculate district emissions**", (5) "**Grid4AQM**", and (6) "**Plot figures**".
411 The main purpose of modularizing the CARS is to meet the needs of various communities, such
412 as policymakers, stakeholders, and air quality modelers. While modules (1) through (4) are

413 required to develop the district-level and road link-level emissions inventories, module (5)
414 "**Grid4AQM**" is optional depending on if users want to develop chemically-speciated gridded
415 hourly emissions for CTMs. Also, the modularity system in the CARS allows users to bypass
416 certain modules if it has been previously processed without any changes. For example, if there is
417 no change in traffic activity, emission factors table, or GIS shapefiles, users do not need to run
418 these modules and can simply read the data frame outputs and then run "**Grid4AQM**" for the
419 modeling dates and domain. The "**Grid4AQM**" module will not only improve the computational
420 time for CTMs but also eliminate the need for a 3rd party emissions modeling system like SMOKE
421 (Baek and Seppanen, 2021).

422   The rectangle boxes in Fig. 5 represent the data array and the boxes with rounded edges are
423 the functions in the CARS. Details on the CARS code, input table format, and functions setup
424 information can be found on the CARS GitHub website (Pedruzzi *et al*., 2020).

425   The "**Process activity data**" module first reads the vehicle activity data, such as an
426 individual vehicle's daily total VKT based on its registered district. The "**Process emission factors**"
427 module reads and stores the emission factors table that holds all pollutant emission factors to
428 estimate the emissions for all vehicles. Meteorology-sensitive emission factors are only limited to
429 NO_x pollutants. District boundary GIS shapefiles and road network shapefiles are processed
430 through "**Process shape file**" to generate the VKT-based redistribution weighting factors from Eq.
431 (13), (14) and (15) for the "**Calculate district emissions**" module to compute district-level and
432 road link-level emission rates (metric tons per year, t yr^{-1}).

433   The redistributed emission rates (t yr^{-1}) from the "**Calculate district emissions**" module
434 present annual total emission rates until district-level VKTs from the "**Process activity data**"
435 module are added. Then, the "**Grid4AQM**" module can generate CTM-ready chemically speciated
436 emissions. The "***Read_chemical***" function from the "**Grid4AQM**" module is designed to process
437 the chemical speciation profile that can convert the inventory pollutants such as CO, NO_X, SO_2,
438 PM_{10}, $PM_{2.5}$, VOC, and NH_3, into the chemically lumped model species that CTM requires for
439 chemical mechanisms, such as SAPRC (L. and Heo, 2012) and Carbon Bond version 6 (CB6)
440 (Yarwood and Jung, 2010). The "***Read_temporal***" function processes the complete set of monthly,
441 weekly, and hourly temporal allocation profiles that can convert annual total emissions to hourly
442 emissions. "***Read_griddesc***" defines the CTM-ready modeling domain and computes the gridding
443 fractions for all road link-level emissions by overlaying the modeling domain over the GIS
444 shapefiles. Once annual total emissions are chemically speciated, spatially gridded, and temporally
445 allocated into hourly emissions, the "***Gridded_emis***" function will combine emission source-level
446 conversion fractions from each function (***Read_chemical***, ***Read_temporal***, and ***Read_griddesc***) to
447 generate the CTM-ready chemically speciated, gridded hourly emissions in the NetCDF binary
448 format. The "**Plot Figures**" module is designed for generating various summary reports and
449 graphics to assist users in understanding the estimated automobile emissions inventory computed

450   by the CARS. The following section will describe the detailed processes of the "**Grid4AQM**"
451   module, which includes chemical, spatial, and temporal allocations.

452   The influence of temperature on emission processes are considered in the CARS model.
453   There are three temperature parameters in current CARS model such as "temp_max" for maximum
454   temperature, "temp_mean" for mean temperature, and "temp_min" for minimum temperature.
455   These temperature parameters will be applied to over the entire modeling domain during the
456   simulation period. Current CARS model version does not support to process gridded meteorology
457   data from the 3rd party meteorology models like Meteorology-Chemistry Interface Processor
458   (MCIP) from U.S. EPA., and Weather Research Forecasting (WRF) model from National Center
459   for Atmospheric Research (NCAR) yet. However, CARS can easily adopt various temporally
460   resolved temperature values by adjusting the CARS simulation period (i.e., day, week, month,
461   season, or annual).

462   **3.1   Chemical Speciation**

463   To support CTMs applications, the CARS needs to be able to convert inventory pollutants
464   into chemical lumped model species based on the choice of CTM chemical mechanisms. NO_x
465   includes nitric oxide (NO), nitrogen dioxide (NO_2), and nitrous acid (HONO). VOCs can represent
466   hundreds of different organic carbon species, such as benzene, acetaldehyde, and formaldehyde.
467   These grouped inventory pollutants cannot be directly imported into the chemical mechanism
468   modules in the CTM system and require chemical speciation allocation for CTMs to process them
469   during their chemical reactions. Therefore, the "**Grid4AQM**" module performs the chemical
470   species allocation step prior to the temporal and spatial allocations to generate the gridded hourly
471   emissions. The "*Read_chemical*" function in "**Grid4AQM**" module allows users to assign these
472   emission inventory pollutants to CTM-ready surrogate chemical species (a.k.a lumped chemical
473   species) by vehicle, engine, and fuel type. For example, VOC emissions from diesel busses can be
474   converted into the following composition based on its chemical allocation profile: alkanes (68%),
475   toluene (9%), xylenes (8%), alkenes (4%), ethylene (2%), benzene (1.3%), and unreactive
476   compounds (7%) when CB6 chemical mechanism is selected. Further details on the chemical
477   speciation profile input formats are available in the CARS user's guide.

478   **3.2   Spatial Allocation**

479   The "**Calculate district emissions**" module calculates not only the total district emissions
480   but also road link-specific emissions based on road link-specific AADT data from road network
481   GIS shapefiles. The "**Calculate district emissions**" module first gets the district total vehicle
482   emissions (Eq. 2) based on the district-level VKTs, and then the normalized district total emissions
483   by district weight factor, ω_d (Eq. 13). Afterwards, the normalized district total emissions are
484   redistributed into every road link using road link-level weight factors ($\omega_{d,l}$) (Eq. 15). The district

485 total emissions from Eq. (2) and from Eq. (15) remain the same. Then the computed road link-
486 level emissions then will be converted into grid cell emissions using the modeling domain grid cell
487 fractions computed in the "***Read_griddesc***" function in the "**Grid4AQM**" module.

488 **3.3 Temporal Allocation**

489 Once chemical and spatial allocations are completed, the final step to support CTM
490 application is a temporal allocation that converts the annual total emissions from the "**Calculate**
491 **district emissions"** module into hourly emissions. The "***Read_temporal***" temporal allocation
492 function in the "**Grid4AQM"** module converts the annual emission rate (t yr^{-1}) to the hourly
493 emission rate (mol hr^{-1}) using monthly, weekly, and weekday/weekend diurnal temporal profiles.
494 This module processes these temporal profile inputs, which are the monthly (January - December),
495 weekly (Monday - Sunday), and weekday/weekend 24 hour profile tables (0:00-23:00 LST). The
496 users can assign these temporal profiles with a combination of vehicle, engine, fuel, and road types
497 to enhance their temporal representations in detail.

498 **3.4 Chemical Transport Model Emissions**

499 The main goal of the **"Grid4AQM"** module is to generate temporally, chemically, and
500 spatially enhanced CTM-ready gridded hourly emissions. First, it reads the CTM modeling domain
501 configuration and then overlays it over the road network GIS shapefile and district-boundary
502 shapefile to define the modeling domain. This overlaying process between the road network,
503 district boundary GIS shapefiles, and modeling domain allows the **"Grid4AQM"** module to
504 compute the fraction of road links that intersects with each grid cell. Figure 6 demonstrates how
505 the district boundary and road network GIS shapefiles are used to perform the spatial allocation
506 processes in CARS. Figure 6a is a native road link shapefile of Seoul with AADT, VKT, district
507 ID, and road type. Figure 6b presents an overlay of two districts's road links (purple and blue) over
508 the selected region. State total emissions will be renormalized into weighed district total emission
509 data and then redistributed into the road link. Figure 6c illustrates how the weighted road link-
510 level emissions get allocated into modeling grid cells for CTMs. The link-level VKT ($VKT_{d,r,l}$)
511 from Eq. (12) will be used to compute a total of traffic activity fractions by grid cell and then use
512 that to assign the link-level emissions from Eq. (2) into each grid cell. When a road link intersects
513 with multiple grid cells, the "**Grid4AQM"** module will weigh the emissions by the length of the
514 link that intersects with each grid cell. It should be noted that current CARS model can only
515 generate the Community Multiscale Air Quality (CAMQ)-ready gridded hourly emissions in
516 format of IOAPI (Input/Output Applications Programming Interface) based on NetCDF format.

517 Through the overlay process, the CARS model can generate various types of output data,
518 such as total district emissions, link-level emissions, and CTM-ready gridded emissions. For
519 example, the CO vehicle emissions from the Seoul metropolitan in South Korea are presented in

520 three different output formats in Fig. 7. Figure 7a shows the annual mobile $PM_{2.5}$ emissions by
521 district. The road link level annual emissions are presented in Fig. 7b. Furthermore, the CARS
522 applies the link-level emissions from Fig. 7b to generate the hourly grid cell emission data with a
523 1 km × 1 km resolution for the CTM in Fig. 7c.

524 **3.5   National Control Strategy Application**

525   One of the unique features in the CARS compared to other mobile emissions models is that
526 it can promptly develop controlled mobile emissions responding to the national emergency high
527 $PM_{2.5}$ episodes. It is very common to experience high $PM_{2.5}$ episodes, especially during the
528 wintertime in South Korea due to domestic and international primary and secondary air pollutants
529 emissions. When the 72 hour forecasted $PM_{2.5}$ concentration exceeds the average 50 µg/m^3 (0:00-
530 16:00 LST), the national $PM_{2.5}$ emergency control strategy is activated for ten days. It applies a
531 nationwide vehicle restriction policy within 24 hours. It enforces a limit on what kind of vehicles
532 can be operated on a certain date. The restrictions can be applied in the following ways: the
533 closures of public parks and government facilities, and restrictions of certain vehicles based on
534 their fuel type and age, which is a major factor of engine deterioration. This policy will limit the
535 number of vehicles on the network roads significantly, which could reduce primary $PM_{2.5}$ and
536 precursor pollutant (NOx, NH_3, and VOC) emissions, especially from heavily populated
537 metropolitan regions (Choi et al., 2014; Kim et al., 2017a; Kim et al., 2017b; Kim et al., 2017c).
538   To understand the impacts of an even/odd vehicle restriction policy in real-time, we need to
539 quickly develop a rapid control response emissions for the air quality forecast modeling system.
540 The process of generating the controlled mobile emissions can take a long time if we start fresh.
541 Thus, we have implemented this control strategy as an optional "*Control Factors*" function in the
542 "**Calculate district emissions"** in the module for users to quickly and easily generate the
543 controlled mobile emissions with consideration of the limited number of vehicles based on the
544 vehicle, engine, fuel, and vehicle manufactured year. A one hundred percent (100%) control factor
545 means that there are no emissions from those selected vehicles.

546   Because of the modularization system in the CARS, we can bypass some computationally
547 expensive data processing modules (i.e., "**Process activity data**", "**Process emission factors**",
548 and "**Process shape file**") and let the "**Calculate district emissions**" module quickly apply control
549 factors while it computes the district-level mobile emission inventory from Eq. (2). This will allow
550 users to reduce the computational time to generate the controlled mobile emissions under a specific
551 control scenario and develop the controlled CTM-ready gridded hourly emissions using the
552 **"Grid4AQM"** module.

3.6 Computational Time

While the CARS can generate a high-quality spatiotemporal emission inventory for policymakers, stakeholders, and air quality modelers, it is quite critical for the CARS to generate these complex mobile emissions effectively and accurately without being at the expense of computational time. This is especially important to meet the needs for an air quality forecast modeling system responding to a national emergency control strategy implementation.

In this section, we will discuss the details of the CARS computational modeling performance. While the CARS model has been highly optimized, the modularization of CARS has also improved its modeling performance with optional module runs. The breakdown of module-specific computational time estimates based on the benchmark CARS runs are listed in Table 1. The benchmark CARS case includes a total of 24,383,578 daily VKT datasets from KSTA over two different years, 84,608 emission factors for all pollutants across a combination of vehicle-age-engine-fuel types, 385,795 road links from the GIS road network shapefiles, 5,150 districts/16-states boundary GIS shapefile, and 5,494 grid cells (=82 rows and 67 columns) for CTMs. Without any computational parallelization, the total processing time of all six modules usually takes around a half hour to generate a single day CTM-ready gridded hourly emission file. However, it can be further shortened to 25-30 minutes on a higher performance computer. Because of the modular system implemented in the CARS, generating one month (31 days) long gridded hourly emissions from CTMs do not require over 15 computational hours, but only around 100 minutes on high-performance computers. The maximum usage of RAM can reach up to 11 GB. Table 1 shows the breakdown of computational time by each module from two different hardwares (desktop and laptop computers). The numbers in parentheses beside the **"Grid4AQM"** module is the computational time for a single day versus 31 days. While the **"Grid4AQM"** module takes an average of 4.9 minutes for a single day emissions generation, processing a consecutive 31 days saves 46% more time, decreasing from 151.9 minutes (=4.9 minutes * 31 days) to 81.6 minutes.

4   Results

CARS and CAPSS Comparison

The CARS model calculates the 2015 onroad automobile emissions based on the latest 2015 emission factors and the 2015-2017 vehicle activity database in South Korea. The annual total emissions from CARS are compared against the ones from NIER CAPSS in Table 2. The CARS model estimated the following annual total emissions in units of metric tons per year (t yr^{-1}): NO_x (301,794); VOC (61,186); CO (373,864), NH_3 (12,453); $PM_{2.5}$ (10,108), and SO_x (172.0). Compared to NIER CAPSS, the CARS overestimated all pollutants except for NO_x (-18% decrease) and SO_x (-17% decrease). It overestimated the emissions of VOC by 33%, $PM_{2.5}$ by 15%, CO by 52%, and NH_3 by 24%. Both NIER CAPSS and CARS shared the same emission factor tables,

588   which hold over 84,608 emission factors for all pollutants across a combination of vehicle, age,
589   engine, and fuel types.

590   The difference between CAPSS and CARS approaches are caused by three reasons: First,
591   the number of vehicles used in CARS is slightly higher (6%) than CAPSS data (1.3 out of 23
592   million), as well as other key traffic-related activity inputs (i.e., vehicle age distribution, averaged
593   speed distribution, etc). Secondly, the vehicle speed information assigned by vehicle and road type
594   play a critical role in the differences between CAPSS and CARS. The CAPSS calculation was
595   based on the road-specific mean speed value or 80% of the speed limit as an input of vehicle
596   operating speed by three road types (rural, urban, and expressway). In other words, CAPSS only
597   assigns a "single-speed value" for each road type, and does not encounter the variation of vehicle
598   speed during its operation on roads into the emissions calculation. Most running exhaust emissions
599   occur during a vehicle's low-speed operation due to its incomplete combustion of fuel, and it is
600   critical to accurately represent the emissions across various speed bins in order to compute the
601   correct emissions. The CARS model has an option to apply the average speed distribution (ASD)
602   over 16 speed bins for eight road types (Fig. 4). The CARS speed distribution process can better
603   represent the speed variations of vehicle speeds for each road type. A detailed analysis of the
604   impact of vehicle speed will be discussed later in this chapter. Lastly, other advanced processes in
605   the CARS, such as link-level AADT and district-level vehicle data (5,150 districts in South Korea),
606   can reflect more spatial detail and variation than the CAPSS. The CAPSS only considers state-
607   level data (17 states in South Korea) and five road types (interstate expressway, urban highway,
608   rural highway, urban local, and rural local).

609   Figure 8 illustrates more details about the difference between the annual emissions from
610   CARS to the CAPSS by pollutants and vehicle types. Sedan vehicles show the largest increase of
611   VOC (33%), CO (41%), and NH_3 (23%) in the CARS relative to CAPSS because almost 56% of
612   total vehicle count (13.5 million) is composed of sedan vehicles. Also, sedan vehicles contribute
613   51% of total VOC and 61% of total CO annual emissions. The VOC and CO emissions from sedans
614   are largely affected by the average speed distribution process when compared to other vehicle
615   types. Similarly, the largest decreases of NO_x (-16%) and SO_x (-18%) are from trucks because they
616   are significant NO_x (~50%) and SO_x contributors (~27%) and their emission factors are sensitive
617   to vehicle speed.

618   **Onroad Emissions Analysis**

619   The CARS is a bottom-up emissions model, which utilizes local individual vehicle activity
620   data, detailed local emission factors for every vehicle and fuel type, and localized inputs such as
621   average speed distribution by road type and deterioration factor. It allows users to assess the
622   detailed breakdown of localized emission contributions. Table 3 represents the individual air
623   pollutants (NO_x, VOC, $PM_{2.5}$, CO, NH_3, and SO_x) emission contributions (t yr^{-1}), fractions (%),

624 and impact factors (IF) by the vehicle type and fuel system. The IF is defined by the normalized
625 annual emissions with vehicle counts of each category (kg yr^{-1} per vehicle). The CARS also can
626 provide the average daily VKT per vehicle, which is the total daily VKT divided by vehicle
627 numbers, to explain the emission contributions in Appendix D.

628   Diesel-fueled vehicles contribute the most of NO_x emissions, which is over 85.3% (257,305
629 t yr^{-1}), although the number of diesel vehicles only amounts to approximately 35% of the total
630 vehicles (Table 3a). While the diesel trucks emitted 49.1% (148,246 t yr^{-1}) of total NO_x with an IF
631 value of 47.9 (kg yr^{-1}), the highest impact (IF = 340 kg yr^{-1}) occurred from diesel buses with only
632 a 8.51% contribution to the total NOx emissions. This is caused by the highest average daily VKT
633 from diesel buses compared to other vehicles, which is expected in a highly populated metropolitan
634 area like Seoul, South Korea. A diesel bus generally has a 3-5 times higher daily VKT (180 km d^{-1}
635) than other common vehicles (gasoline sedan: 34 km d^{-1}, diesel truck: 57 km d^{-1}). The second-
636 largest vehicle type is the CNG (compressed natural gas) bus (248 kg yr^{-1}), which also has a higher
637 VKT. Their average daily VKT is 212 km d^{-1}, with only a 3.1% NO_x contribution.

638   For VOC emissions, over 12 million gasoline vehicles cause 52.1% (31,885 t yr^{-1}) of the
639 total VOC emissions, and the gasoline sedan is the highest contributor across all vehicle types,
640 which is over 28,434 t yr^{-1} (46.5%) (Table 3b). Unlike NOx emissions, diesel vehicles only
641 contribute 23.0% (14,070 t yr^{-1}) of the total VOC emissions. Across the vehicle fuel types, the IF
642 outcome indicates that CNG vehicles have the highest IF values for VOC, which is 247 kg yr^{-1} due
643 to the relatively high VOC contribution (19% over total VOC) and a low number of heavy CNG
644 vehicles. The IF of CNG trucks are 77.2 kg yr^{-1}, but only contribute 0.2% to total VOC emissions.
645 The IF of the CNG bus is 320 kg yr^{-1} and emits 19.5% of the total VOC. Comparing the IFs of
646 buses across fuel types, the CNG bus emits less NO_x but higher VOC than a diesel vehicle. Each
647 CNG bus has about 33 times higher IF of VOC (320 kg yr^{-1}) than a diesel bus (9.51 kg yr^{-1}), and
648 CNG buses released slightly lower NO_x (248 kg yr^{-1}) than diesel buses (340 kg yr^{-1}) (Table 3a and
649 3b).

650   The current South Korea NIER currently does not have the PM emission factors from tire
651 and brake wear, which are the highest contributors of $PM_{2.5}$ emissions from onroad vehicles (Hugo
652 A.C. et al., 2013; Fulvio Amato et al., 2014). Once the emission factors of tire and brake wear are
653 prepared, those emissions can be computed by CARS. For that reason, diesel vehicles become the
654 major source of $PM_{2.5}$ emissions, which contributes over 98.5% (9,959 t yr^{-1}) of the $PM_{2.5}$
655 emissions based on the CARS 2015 emissions (Table 3c). The diesel truck, SUV, and van are the
656 three major sources, and their contributions of total $PM_{2.5}$ are 53.6%, 21.4%, and 11.2%,
657 respectively. Although over 52% of the vehicles are gasoline vehicles, their primary $PM_{2.5}$
658 contribution is limited to 1.44%. The diesel bus has the highest IF (2.83 kg yr^{-1}), which is caused
659 by the largest average daily VKTs.

Similar to VOC emissions, CO is mostly emitted through the tailpipe due to incomplete internal combustion of fuel and share similar emissions distributions across vehicle and fuel types (Table 3d). Gasoline vehicles contribute most of the CO (220,390 t yr^{-1}, 59.0%), and sedan vehicles are the primary source (178,121 t yr^{-1}, 47.6%) of this out of all gasoline vehicles. Across vehicle types, bus shows the highest IF of CO (81.2 kg yr^{-1}) due to its largest daily VKT. CO is the most abundant pollutant released from vehicles (373,864 t yr^{-1}) across all pollutants from onroad automobile sources. Although CO is much less reactive than other vehicle VOCs (Rinke and Zetzsch, 1984; Liu and Sander, 2015), the majority of CO emissions from onroad automobile sources plays a critical role in generating 30% of hydroperoxyl radicals (HO$_2$) and causing ozone formation in urban areas (Pfister et al., 2019). Thus, CO is also another crucial precursor to ozone formation in urban areas.

SO$_x$ emissions are related to the sulfur content within the fuel component; diesel has a higher sulfur content than any other fuels. Most SO$_x$ is contributed by diesel vehicles (93.8 t yr^{-1}, 54.5%) (Table 3e). Within diesel vehicles, trucks provide 26.5% of SO$_x$ (45. t yr^{-1}). Although the SO$_x$ from sedan vehicles are slightly higher (~3.3%) than diesel trucks, the number of diesel trucks is only 29.6% of the number of gasoline sedans. Thus, diesel trucks have a higher IF than gasoline sedans. Across vehicle types, buses have the highest IF (0.095 kg yr^{-1}) of SO$_x$, and diesel buses in particular have the largest IF at 0.143 kg yr^{-1}.

The NH$_3$ emissions table (table 3f) indicates that 98.7% of NH$_3$ is from gasoline vehicles while diesel trucks only contribute 1.13%. The IF result also shows that the gasoline sedan has the most significant impact per vehicle (1.17 kg yr^{-1}).

According to the vehicle activity and the CARS model results, nearly half of the total vehicles (24.3 million) are gasoline sedans (10.4 million, 42.8%), and gasoline sedan vehicles contributed most of the VOC and CO emissions (46.5% and 47.6%), but only 7.7% of the total NO$_x$ emissions. The number of diesel vehicles is 8.6 million (35.4%); however, they emitted about 85.3% of the total NO$_x$ and 98.5% of the primary PM$_{2.5}$. These results indicated that the annual traffic-related mobile emissions are not only affected by the number of vehicles, but also by different vehicle and fuel types. Therefore, this study normalized the annual emissions by the number of vehicles to confirm the emission composition by individual vehicle types.

Average Speed Impact Study

The CARS can also optionally apply the average speed distribution (ASD) by road type to compute more realistic mobile emissions on the road network when compared to using a current single average speed value for each road type (Appendix E). Applying the ASD will generate a better representation of actual traffic patterns from each road type. To understand the impacts of ASD application, we performed sensitivity runs between using a single-speed to the ASD application (Appendix F). The ASD data was described in Fig. 4, and the road-specific average

696 single-speed values were developed based on the weighted average method using the same ASD
697 data. Appendix E and S6 describe the details of ASD as well as road-specific speed values.

698   Figure 9a shows the differences in total emissions between two scenarios and is organized
699 by pollutant. The single-speed scenario largely underestimates the emissions across all pollutants
700 compared to the ones from the ASD scenario. NO_x (16%), VOC (40%), and CO (30%) were
701 especially underestimated. The difference is caused by the lack of low-speed bins (<16 km h^{-1})
702 representation when a single average speed approach was used. Higher emissions are emitted while
703 vehicles are operated with low-speed bins, which decreases the combustion efficiency of ICE and
704 releases more pollutants.

705   Figure 9b shows the road-specific breakdown between the ASD and single speed scenarios
706 to understand the impacts of vehicle operating speeds on onroad automobile emissions. In this
707 figure, each color indicates the emissions percentage differences by road types. Other than NH_3,
708 significant discrepancies happened between local urban roads (5.8%), highways (3.9%), and urban
709 highways (3.0%). Other pollutants, VOC, $PM_{2.5}$, CO, and SO_x, have similar fractions of road types.
710 This phenomenon is caused by low-speed conditions (<16 km h^{-1}) and the fractions of road VKT
711 contributions (Appendix C). The lower speeds cause the incomplete combustion of ICE and
712 increase the emission rate. Also, local urban roads, highways, and urban highways have higher
713 road VKT contributions at 17%, 18%, and 12%, respectively (Appendix C) than rural roads.
714 Higher emissions from low speed conditions from these high contribution roads (urban local, urban
715 highway, and highway) caused these significant differences between the ASD and single-speed
716 approaches. Although the interstate expressway has the largest VKT contribution (41%), it also
717 has the lowest fraction of low-speed bins (2%). That is why the difference between the ASD and
718 single speed scenarios on interstate expressways is less than 1%. In general, NH_3 emission factors
719 do not change by vehicle operating speed, so the ASD impact is quite minimal.

5   Conclusions

721   The CARS is a bottom-up automobile emissions model that utilizes the localized traffic-
722 related activity and emission factors input datasets to generate high quality localized bottom-up
723 emissions inventories for policymakers, stakeholders, and research community as well as
724 temporally and spatially enhanced hourly gridded emissions for CTMs. First, the CARS model
725 employs the daily VKTs for all registered vehicles and the emission factors function to compute
726 district-level total daily emissions for each vehicle. To reflect realistic traffic patterns, the CARS
727 model computes and utilizes link-level VKTs (=link-length×AADT) from the road network GIS
728 shapefiles to redistribute the original district-level total emissions into spatially enhanced road
729 link-level emissions. It can also optionally implement a control strategy as well as road restriction
730 rules to improve the quality of local emission inventories and meet the needs of users.

731 The CARS model is a fully modularized and computationally optimized python-based
732 bottom-up mobile emissions model that can effectively process a huge dataset to calculate high
733 quality spatiotemporal county-level, road link-level and grid cell-level mobile emissions. We
734 believe that the implementation of the ASD into the CARS improves the representation of onroad
735 automobile emissions from the road network when compared to a single-speed for each road type
736 approach. It allows the CARS to have a better representation of low speed (<16 km h-1) vehicle
737 emissions. We believe that CARS model's versatile spatiotemporal bottom-up automobile
738 emissions and the in-depth analysis feature can assist government policymakers and stakeholders
739 to develop the rapid responsive emission abatement strategies as a response to the South Korea's
740 national PM$_{2.5}$ emergency control strategy that enforces the nationwide vehicle restriction policy
741 within 24 hours.

Code Availability:

743 The source code of the CARS model public release version 1.0 can be downloaded from the
744 Github release website:

745 https://github.com/bokhaeng/CARS/releases/tag/CARSv1.0
746
747

Digital Object Identifier (DOI) for the CARS version 1.0:

749 https://zenodo.org/record/5033314#.YNzDrC1h001
750
751

Installation Package for CARS version 1.0:

753 The CARS version 1.0 installation package comes with the complete inputs and outputs datasets
754 for users to confirm their proper installation on their computers and can be downloaded from the
755 Github release website:

756 https://github.com/bokhaeng/CARS/releases/download/CARSv1.0/CARS_v1.0_public_release_
757 package_25June2021.zip
758
759

User's Guide Documentation:

761 The CARS version user's guide documentation can be accessed through the Github repository:

762 https://github.com/bokhaeng/CARS/tree/master/docs/User_Manual
763
764

Data availability:

All the datasets, excel and python scripts used in this manuscript for the data analysis are uploaded through GMD website along with a supplemental appendix document.

Author contribution

Dr. B.H. Baek and Dr. Jung-Hun Woo are lead researchers in this study. Dr. Rizzieri Pedruzzi develop the source code of CARS model, Dr. Minwoo Park tested the model and provided the model input data. Dr. Chi-Tsan Wang analyzed the model result and prepared the manuscript. Younha Kim, Chul-Han Song, analyzed the model result and provided comments.

Competing interests

The Authors declare that they have no conflict of interest.

Acknowledgments

This research was funded by the National Strategic Project-Fine Particle of the National Research Foundation (NRF) of Korea funded by the Ministry of Science and ICT (MSIT), the Ministry of Environment (ME), the Ministry of Health and Welfare (MOHW) (NRF-2017M3D8A1092022), and by the Korea Environmental Industry & Technology Institute (KEITI) through the Public Technology Program based on Environmental Policy Program, funded by Korea Ministry of Environment (MOE) (2019000160007).

References

Safety flare for burning combustible gas - has tangential inlet for non-flammable gas between housing and stack, in, Shell Oil Co (Shel-C).

Anaconda, Anaconda python: https://www.anaconda.com/products/individual, last access: May, 1st, 2020.

Appel, W., Chemel, C., Roselle, S., Francis, X., Hu, R.-M., Sokhi, R., Rao, S. T., and Galmarini, S.: Examination of the Community Multiscale Air Quality (CMAQ) model performance over the North American and European domains, Atmospheric Environment, 53, 142–155, 10.1016/j.atmosenv.2011.11.016, 2013.

Baek, B. H., and Seppanen, C., SMOKE v4.8.1 Public Release (January 29, 2021) (Version SMOKEv481_Jan2021): http://doi.org/10.5281/zenodo.4480334 last 2021.

Burnett, R., Chen, H., Szyszkowicz, M., Fann, N., Hubbell, B., Pope, C. A., Apte, J. S., Brauer, M., Cohen, A., Weichenthal, S., Coggins, J., Di, Q., Brunekreef, B., Frostad, J., Lim, S. S., Kan, H., Walker, K. D., Thurston, G. D., Hayes, R. B., Lim, C. C., Turner, M. C., Jerrett, M., Krewski, D., Gapstur, S. M., Diver, W. R., Ostro, B., Goldberg, D., Crouse, D. L., Martin, R. V., Peters, P., Pinault, L., Tjepkema, M., van Donkelaar, A., Villeneuve, P. J., Miller, A. B., Yin, P., Zhou, M., Wang, L., Janssen, N. A. H., Marra, M., Atkinson, R. W., Tsang, H., Quoc Thach, T., Cannon, J. B., Allen, R. T., Hart, J. E., Laden, F., Cesaroni, G., Forastiere, F., Weinmayr, G., Jaensch, A., Nagel, G., Concin, H., and Spadaro, J. V.: Global estimates of mortality associated with long-term exposure to outdoor fine particulate matter, Proceedings of the National Academy of Sciences, 115, 9592, 10.1073/pnas.1803222115, 2018.

Choi, D., Beardsley, M., Brzezinski, D., Koupal, J., and Warila, J.: MOVES Sensitivity Analysis: The Impacts of Temperature and Humidity on Emissions
, available at: https://www3.epa.gov/ttn/chief/conference/ei19/session6/choi.pdf 2017.

Choi, K.-C., Lee, J.-J., Bae, C. H., Kim, C.-H., Kim, S., Chang, L.-S., Ban, S.-J., Lee, S.-J., Kim, J., and Woo, J.-H.: Assessment of transboundary ozone contribution toward South Korea using multiple source–receptor modeling techniques, Atmospheric Environment, 92, 118-129, https://doi.org/10.1016/j.atmosenv.2014.03.055, 2014.

Cohen, A. J., Brauer, M., Burnett, R., Anderson, H. R., Frostad, J., Estep, K., Balakrishnan, K., Brunekreef, B., Dandona, L., Dandona, R., Feigin, V., Freedman, G., Hubbell, B., Jobling, A.,

817 Kan, H., Knibbs, L., Liu, Y., Martin, R., Morawska, L., Pope, C. A., III, Shin, H., Straif, K.,
818 Shaddick, G., Thomas, M., van Dingenen, R., van Donkelaar, A., Vos, T., Murray, C. J. L., and
819 Forouzanfar, M. H.: Estimates and 25-year trends of the global burden of disease attributable to
820 ambient air pollution: an analysis of data from the Global Burden of Diseases Study 2015, The
821 Lancet, 389, 1907-1918, 10.1016/S0140-6736(17)30505-6, 2017.
822

823 Dennis, R., Fox, T., Fuentes, M., Gilliland, A., Hanna, S., Hogrefe, C., Irwin, J., Rao, S. T.,
824 Scheffe, R., Schere, K., Steyn, D., and Venkatram, A.: A FRAMEWORK FOR EVALUATING
825 REGIONAL-SCALE NUMERICAL PHOTOCHEMICAL MODELING SYSTEMS, Environ
826 Fluid Mech (Dordr), 10, 471-489, 10.1007/s10652-009-9163-2, 2010.

827 EEA: EMEP/EEO air pollutant emission inventory guidebook 2016, 2019.

828 Enthought, Enthought Canapy Python: https://assets.enthought.com/downloads/edm/, last
829 access: May, 1st, 2020.

830 Fallahshorshani, M., André, M., Bonhomme, C., and Seigneur, C.: Coupling Traffic, Pollutant
831 Emission, Air and Water Quality Models: Technical Review and Perspectives, Procedia - Social
832 and Behavioral Sciences, 48, 1794-1804, https://doi.org/10.1016/j.sbspro.2012.06.1154, 2012.

833 Fulvio Amato, Flemming R. Cassee, Hugo A.C. Denier van der Gon, Robert Gehrig, Mats
834 Gustafsson, Wolfgang Hafner, Roy M. Harrison, Magdalena Jozwicka, Frank J. Kelly,
835 TeresaMoreno, Andre S.H. Prevot, Martijn Schaap, Jordi Sunyer, Xavier Querol, Urban air
836 quality:The challenge of traffic non-exhaust emissions, Journal of Hazardous Materials, 275, 31-
837 36, https://doi.org/10.1016/j.jhazmat.2014.04.053, 2014.
838

839 Guevara, M., Tena, C., Porquet, M., Jorba, O., and Pérez García-Pando, C.: HERMESv3, a
840 stand-alone multi-scale atmospheric emission modelling framework – Part 1: global and regional
841 module, Geosci. Model Dev., 12, 1885-1907, 10.5194/gmd-12-1885-2019, 2019.

842 Hogrefe, C., Rao, S. T., Kasibhatla, P., Hao, W., Sistla, G., Mathur, R., and McHenry, J.:
843 Evaluating the performance of regional-scale photochemical modeling systems: Part II—ozone
844 predictions, Atmospheric Environment, 35, 4175-4188, https://doi.org/10.1016/S1352-
845 2310(01)00183-2, 2001a.

846 Hogrefe, C., Rao, S. T., Kasibhatla, P., Kallos, G., Tremback, C. J., Hao, W., Olerud, D., Xiu,
847 A., McHenry, J., and Alapaty, K.: Evaluating the performance of regional-scale photochemical

848   modeling systems: Part I—meteorological predictions, Atmospheric Environment, 35, 4159-
849   4174, https://doi.org/10.1016/S1352-2310(01)00182-0, 2001b.

850   Hugo A.C. Denier van der Gon, Miriam E. Gerlofs-Nijland, Robert Gehrig, Mats Gustafsson,
851   Nicole Janssen, Roy M. Harrison, Jan Hulskotte, Christer Johansson, Magdalena Jozwicka,
852   Menno Keuken, Klaas Krijgsheld, Leonidas Ntziachristos, Michael Riediker & Flemming R.
853   Cassee: The Policy Relevance of Wear Emissions from Road Transport, Now and in the
854   Future—An International Workshop Report and Consensus Statement, Journal of the Air &
855   Waste Management Association, 63:2, 136-149, DOI: 10.1080/10962247.2012.741055, 2013
856

857   Ibarra-Espinosa, S., Ynoue, R., amp, apos, Sullivan, S., Pebesma, E., Andrade, M. d. F., and
858   Osses, M.: VEIN v0.2.2: an R package for bottom–up vehicular emissions inventories, Geosci.
859   Model Dev., 11, 2209-2229, 10.5194/gmd-11-2209-2018, 2018a.

860   Ibarra-Espinosa, S., Ynoue, R., O'Sullivan, S., Pebesma, E., Andrade, M. D. F., and Osses, M.:
861   VEIN v0.2.2: an R package for bottom–up vehicular emissions inventories, Geosci. Model Dev.,
862   11, 2209-2229, 10.5194/gmd-11-2209-2018, 2018b.

863   IEMA, Inventário de Emissões Atmosféricas do Transporte Rodoviário de Passageiros no
864   Município de São Paulo.: http://emissoes.energiaambiente.org.br, last access: May,1st, 2017.

865   Jang, Y. K., Cho, K. L., Kim, K., Kim, H. J., and Kim, J.: Development of methodology for
866   esimation of air pollutants emissions and future emissions from on-road mobile sources.,
867   National Institute of Environmental Research, Incheon, Korea., available at: 2007.

868   Kaewunruen, S., Sussman, J. M., and Matsumoto, A.: Grand Challenges in Transportation and
869   Transit Systems, Frontiers in Built Environment, 2, 10.3389/fbuil.2016.00004, 2016.

870   Kim, B.-U., Bae, C., Kim, H. C., Kim, E., and Kim, S.: Spatially and chemically resolved source
871   apportionment analysis: Case study of high particulate matter event, Atmospheric Environment,
872   162, 55-70, https://doi.org/10.1016/j.atmosenv.2017.05.006, 2017a.

873   Kim, H. C., Kim, E., Bae, C., Cho, J. H., Kim, B. U., and Kim, S.: Regional contributions to
874   particulate matter concentration in the Seoul metropolitan area, South Korea: seasonal variation
875   and sensitivity to meteorology and emissions inventory, Atmos. Chem. Phys., 17, 10315-10332,
876   10.5194/acp-17-10315-2017, 2017b.

877 Kim, H. C., Kim, S., Kim, B.-U., Jin, C.-S., Hong, S., Park, R., Son, S.-W., Bae, C., Bae, M.,
878 Song, C.-K., and Stein, A.: Recent increase of surface particulate matter concentrations in the
879 Seoul Metropolitan Area, Korea, Scientific Reports, 7, 4710, 10.1038/s41598-017-05092-8,
880 2017c.

881 L., W. P., and Heo, G.: Development of revised SAPRC aromatics mechanism, available at:
882 https://www.engr.ucr.edu/~carter/SAPRC/saprc11.pdf 2012.

883 Lee, D., Lee, Y.-M., Jang, K.-W., Yoo, C., Kang, K.-H., Lee, J.-H., Jung, S.-W., Park, J.-M.,
884 Lee, S.-B., Han, J.-S., Hong, J.-H., and Lee, S.-J.: Korean National Emissions Inventory System
885 and 2007 Air Pollutant Emissions, Asian Journal of Atmospheric Environment, 5-4, 278-291,
886 2011a.

887 Lee, D.-G., Lee, Y.-M., Jang, K.-W., Yoo, C., Kang, K.-H., Lee, J.-H., Jung, S.-W., Park, J.-M.,
888 Lee, S.-B., Han, J.-S., Hong, J.-H., and Lee, S.-J.: Korean National Emissions Inventory System
889 and 2007 Air Pollutant Emissions, Asian Journal of Atmospheric Environment, 5,
890 10.5572/ajae.2011.5.4.278, 2011b.

891 Lejri, D., Can, A., Schiper, N., and Leclercq, L.: Accounting for traffic speed dynamics when
892 calculating COPERT and PHEM pollutant emissions at the urban scale, Transportation Research
893 Part D: Transport and Environment, 63, 588-603, https://doi.org/10.1016/j.trd.2018.06.023,
894 2018.

895 Li, F., Zhuang, J., Cheng, X., Li, M., Wang, J., and Yan, Z.: Investigation and Prediction of
896 Heavy-Duty Diesel Passenger Bus Emissions in Hainan Using a COPERT Model, Atmosphere,
897 10, 106, 10.3390/atmos10030106, 2019.

898 Li, Q., Qiao, F., and yu, L.: Vehicle Emission Implications of Drivers Smart Advisory System
899 for Traffic Operations in Work Zones, Journal of the Air & Waste Management Association, 11,
900 10.1080/10962247.2016.1140095, 2016.

901 Liu, H., Guensler, R., Lu, H., Xu, Y., Xu, X., and Rodgers, M.: MOVES-Matrix for High-
902 Performance On-Road Energy and Running Emission Rate Modeling Applications, Journal of
903 the Air & Waste Management Association, 69, 10.1080/10962247.2019.1640806, 2019.

904 Liu, Y., and Sander, S. P.: Rate Constant for the OH + CO Reaction at Low Temperatures, The
905 Journal of Physical Chemistry A, 119, 10060-10066, 10.1021/acs.jpca.5b07220, 2015.

906   Luo, H., Astitha, M., Hogrefe, C., Mathur, R., and Rao, S. T.: A new method for assessing the
907   efficacy of emission control strategies, Atmospheric Environment, 199, 233-243,
908   https://doi.org/10.1016/j.atmosenv.2018.11.010, 2019.

909   Lv, W., Hu, Y., Li, E., Liu, H., Pan, H., Ji, S., Hayat, T., Alsaedi, A., and Ahmad, B.: Evaluation
910   of vehicle emission in Yunnan province from 2003 to 2015, J. Clean Prod., 207, 814-825,
911   https://doi.org/10.1016/j.jclepro.2018.09.227, 2019.

912   Moussiopoulos, N., Vlachokostas, C., Tsilingiridis, G., Douros, I., Hourdakis, E., Naneris, C.,
913   and Sidiropoulos, C.: Air quality status in Greater Thessaloniki Area and the emission reductions
914   needed for attaining the EU air quality legislation, Sci. Total Environ., 407, 1268-1285,
915   https://doi.org/10.1016/j.scitotenv.2008.10.034, 2009.

916   Nagpure, A. S., Gurjar, B. R., Kumar, V., and Kumar, P.: Estimation of exhaust and non-exhaust
917   gaseous, particulate matter and air toxics emissions from on-road vehicles in Delhi, Atmospheric
918   Environment, 127, 118-124, 10.1016/j.atmosenv.2015.12.026, 2016.

919   NIER: Study on Air Pollutant Emission Estimation Method in Transportation section(II) 11-
920   1480523-003573-01, National Archives of Korea, available at:
921   https://www.archives.go.kr/next/manager/publishmentSubscriptionDetail.do?prt_seq=114054&p
922   age=1554&prt_arc_title=&prt_pub_kikwan=&prt_no 2018.

923   Ntziachristos, L., and Samaras, Z.: Speed-dependent representative emission factors for catalyst
924   passenger cars and influencing parameters, Atmospheric Environment, 34, 4611-4619,
925   https://doi.org/10.1016/S1352-2310(00)00180-1, 2000.

926   Ntziachristos, L., Gkatzoflias, D., Kouridis, C., and Samaras, Z.: COPERT: A European road
927   transport emission inventory model, 491-504 pp., 2009.

928   Pedruzzi, R., Baek, B. H., and Wang, C.-T., CARS: https://github.com/CMASCenter/CARS,
929   last access: MAy, 1st, 2020.

930   Perugu, H., Ramirez, L., and DaMassa, J.: Incorporating temperature effects in California's on-
931   road emission gridding process for air quality model inputs, Environ Pollut, 239, 1-12,
932   10.1016/j.envpol.2018.03.094, 2018.

933   Perugu, H.: Emission modelling of light-duty vehicles in India using the revamped VSP-based
934   MOVES model: The case study of Hyderabad, Transportation Research Part D: Transport and
935   Environment, 68, 150-163, https://doi.org/10.1016/j.trd.2018.01.031, 2019.

936   Pfister, G., Wang, C.-t., Barth, M., Flocke, F., Vizuete, W., and Walters, S.: Chemical
937   Characteristics and Ozone Production in the Northern Colorado Front Range, JGR, 2019.

938   Pinto, J. A., Kumar, P., Alonso, M. F., Andreão, W. L., Pedruzzi, R., dos Santos, F. S., Moreira,
939   D. M., and Albuquerque, T. T. d. A.: Traffic data in air quality modeling: A review of key
940   variables, improvements in results, open problems and challenges in current research,
941   Atmospheric Pollution Research, 11, 454-468, https://doi.org/10.1016/j.apr.2019.11.018, 2020.

942   Rao, S. T., Galmarini, S., and Puckett, K.: Air Quality Model Evaluation International Initiative
943   (AQMEII): Advancing the State of the Science in Regional Photochemical Modeling and Its
944   Applications, Bulletin of the American Meteorological Society, 92, 23-30,
945   10.1175/2010BAMS3069.1, 2011.

946   Rodriguez-Rey et al. (2021): Rodriguez-Rey, D., Guevara, M., Linares, MP., Casanovas, J.,
947   Salmerón, J., Soret, A.,Jorba, O., Tena, C., Pérez García-Pando, C.: A coupled macroscopic
948   traffic and pollutant emission modelling system for Barcelona, Transportation Research Part D,
949   92, https://doi.org/10.1016/j.trd.2021.102725, 2021.

950   Rinke, M., and Zetzsch, C.: Rate Constants for the Reactions of OH Radicals with Aromatics:
951   Benzene, Phenol, Aniline, and 1,2,4-Trichlorobenzene, Berichte der Bunsengesellschaft für
952   physikalische Chemie, 88, 55-62, 10.1002/bbpc.19840880114, 1984.

953   Russell, A., and Dennis, R.: NARSTO critical review of photochemical models and modeling,
954   Atmospheric Environment, 34, 2283-2324, https://doi.org/10.1016/S1352-2310(99)00468-9,
955   2000.

956   Ryu, J. H., Han, J. S., Lim, C. S., Eom, M. D., Hwang, J. W., Yu, S. H., Lee, T. W., Yu, Y. S.,
957   and Kim, G. H.: The Study on the Estimation of Air Pollutants from Auto- mobiles (I) -
958   Emission Factor of Air Pollutants from Middle and Full sized Buses., in, Transportation
959   Pollution Research Center, National Institute of Environmental Research, Incheon, Korea., 2003.

960   Ryu, J. H., Lim, C. S., Yu, Y. S., Han, J. S., Kim, S. M., Hwang, J. W., Eom, M. D., Kim, G. Y.,
961   Jeon, M. S., Kim, Y. H., Lee, J. T., and Lim, Y. S.: The Study on the Esti- mation of Air
962   Pollutants from Automobiles (II) - Emis- sion Factor of Air Pollutants from Diesel Truck., in,

963   Trans- portation Pollution Research Center, National Institute of Environmental Research,
964   Incheon, Korea., 2004.

965   Ryu, J. H., Yu, Y. S., Lim, C. S., Kim, S. M., Kim, J. C., Gwon, S. I., Jeong, S. W., and Kim, D.
966   W.: The Study on the Estimation of Air Pollutants from Automobiles (III) - Emission Factor of
967   Air Pollutants from Small sized Light-duty Vehicles., in, Transportation Pollution Research
968   Center, National Institute of Environmental Research, Korea., 2005.

969   Sallis, P., Bull, F., Burdett, P., Frank, P., Griffiths, P., Giles-Corti, P., and Stevenson, M.: Use of
970   science to guide city planning policy and practice: How to achieve healthy and sustainable future
971   cities, The Lancet, 388, 10.1016/S0140-6736(16)30068-X, 2016.

972   Smit, R., Kingston, P., Neale, D. W., Brown, M. K., Verran, B., and Nolan, T.: Monitoring on-
973   road air quality and measuring vehicle emissions with remote sensing in an urban area,
974   Atmospheric Environment, 218, 116978, https://doi.org/10.1016/j.atmosenv.2019.116978, 2019.

975   Sun, W., Duan, N., Yao, R., Huang, J., and Hu, F.: Intelligent in-vehicle air quality
976   management : a smart mobility application dealing with air pollution in the traffic, 2016.

977   Tominaga, Y., and Stathopoulos, T.: Ten questions concerning modeling of near-field pollutant
978   dispersion in the built environment, Build. Environ., 105, 390-402,
979   https://doi.org/10.1016/j.buildenv.2016.06.027, 2016.

980   USEPA: Population and Activity of Onroad Vehicles in MOVES3, in, edited by: USEPA, 2020.

981   WHO, Ambient air pollution- a major threat to health and climate:
982   https://www.who.int/airpollution/ambient/en/, last 2019.

983   Xu, X., Liu, H., Anderson, J. M., Xu, Y., Hunter, M. P., Rodgers, M. O., and Guensler, R. L.:
984   Estimating Project-Level Vehicle Emissions with Vissim and MOVES-Matrix, Transportation
985   Research Record, 2570, 107-117, 10.3141/2570-12, 2016.

986   Yarwood, G., and Jung, J.: UPDATES TO THE CARBON BOND MECHANISM FOR
987   VERSION 6 (CB6), 2010.
988

989   **Tables**

990   **Table 1**. Computational processing time by CARS module based on the modeling setup: Total
991   number of activity data = 24,383,578; Emission Factors = 84,608; GIS road links=385,795;
992   districts/states=5,150/16; 9km×9km grid cells=5,494 (82 columns× 67 columns).

No	Module	Desktop i7 (minutes)	Laptop i9 (minutes)	Averaged Time (minutes)
1	**Process activity data**	1.8	1.5	1.7
2	**process emission factors**	1.1	0.8	1.0
3	**Process shape file**	9.9	7.3	8.6
4	**Calculate district emissions**	6.4	5.7	6.1
5	**Grid4AQM** [31days]	4.8 [75.9]	5.0 [87.2]	4.9 [81.6]
6	**Plot figures**	6.2	5.4	5.8
	Total [31days]	30.2 [101.3]	25.7 [107.9]	28.1[104.8]

993
994
995

996 **Table 2**. The total emissions comparison between CARS and CAPSS for the 2015 emission.

Emission Inventory	Pollutants (t yr^{-1})					
	NO$_x$	VOC	PM2.5	CO	SO$_x$	NH$_3$
CARS 2015	**301,794**	**61,186**	**10,108**	**373,864**	**172**	**12,453**
CAPSS 2015	369,585	46,145	8,817	245,516	209	10,079

997

998

999 **Table 3**. The summary tables of emissions (t yr^{-1}), contributions (%), and impact factor (IF, kg yr^{-1})

1000) per vehicle for criteria air pollutants (CAPs) by vehicle and fuel types: (a) for NO$_x$; (b) VOC;

1001 (c) for PM$_{2.5}$; (d) for CO; (e) for SO$_x$; and (f) for NH$_3$.

1002

1003 (a) NOx

Vehicle	Gasoline		Diesel		LPG		CNG		Hybrid		Total	
	Emission	IF	Emission	IF	Emission	IF	Emission	IF	Emission	IF	Emission	IF
Sedan	20,219 (6.70%)	1.94	14,783 (4.90%)	12.8	8,159 (2.77%)	4.49	12 (0.00%)	1.26	65 (0.02%)	0.39	43,239 (14.3%)	3.19
Truck	23 (0.01%)	5.54	**148,246 (49.1%)**	47.9	920 (0.31%)	4.55	88 (0.03%)	66.4	-	-	**149,277 (49.5%)**	45.2
Bus	0 (0.00%)	0.97	25,677 (8.51%)	**340**	-	-	9,260 (3.07%)	248	0 (0.00%)	1.77	34,938 (11.6%)	**333**
SUV	159 (0.05%)	1.19	39,565 (13.1%)	11.4	175 (0.06%)	8.54	0 (0.00%)	1.60	1 (0.00%)	0.42	39,900 (13.2%)	11.0
Van	14 (0.00%)	4.78	16,659 (5.52%)	22.6	1,337 (0.44%)	6.80	0 (0.00%)	1.25	0 (0.00)	0.37	18,012 (6.00%)	19.2
Taxi	-	-	-	-	1,217 (0.40%)	2.11	-	-	-	-	1,217 (0.40%)	2.11
Special	1 (0.00%)	20.1	12,347 (4.10%)	152	0 (0.00%)	0.52	-	-	-	-	12,375 (4.10%)	151
Motorcycle	2,836 (0.94%)	1.31	-	-	-	-	-	-	-	-	2,836 (0.94%)	1.32
Total	23,253 (7.70%)	1.83	**257,305 (85.3%)**	29.9	11,809 (3.91%)	4.20	9,361 (3.10%)	**36.7**	66 (0.02%)	0.39	301,794 (100%)	13.3

1004

1005 (b) VOC

Vehicle	Gasoline		Diesel		LPG		CNG		Hybrid		Total	
	Emission	IF	Emission	IF	Emission	IF	Emission	IF	Emission	IF	Emission	IF
Sedan	28,434 (46.5%)	2.73	629 (1.03%)	0.55	2,107 (3.44%)	1.16	3 (0.01%)	0.33	77 (0.13%)	0.47	**31,250 (51.1%)**	2.30
Truck	23 (0.04%)	5.44	8,194 (13.4%)	2.65	286 (0.47%)	1.41	102 (0.17%)	77.2	-	-	8,605 (14.1%)	2.61
Bus	0 (0.00%)	1.65	717 (1.17%)	9.51	-	-	11,942 (19.5%)	320	0 (0.00%)	0	12,659 (20.7%)	**112**
SUV	246 (0.40%)	1.84	2,441 (3.99%)	0.71	46 (0.08%)	2.25	0 (0.00%)	0.75	1 (0.00%)	0.55	2,733 (4.47%)	0.76
Van	21 (0.03%)	7.04	1,185 (1.94%)	1.61	393 (0.64%)	2.00	0 (0.00%)	0.45	0 (0.00%)	0	1,599 (2.61%)	1.71
Taxi	-	-	-	-	273 (0.45%)	0.47	-	-	-	-	273 (0.45%)	0.47
Special	1 (0.00%)	25.8	904 (1.48%)	11.1	0 (0.00%)	0.23	-	-	-	-	905 (1.48%)	11.0
Motorcycle	3,160 (5.16%)	1.46	-	-	-	-	-	-	-	-	3,160 (5.16%)	1.46
Total	**31,885 (52.1%)**	2.50	14,070 (23.0%)	1.64	3,106 (5.08%)	1.10	12,047 (19.7%)	**247**	78 (0.13%)	0.47	61,186 (100%)	2.51

1006

1007 (c) PM2.5

Vehicle	Gasoline		Diesel		LPG		CNG		Hybrid		Total	
	Emission	IF	Emission	IF	Emission	IF	Emission	IF	Emission	IF	Emission	IF
Sedan	144 (1.42%)	0.01	809 (8.00%)	0.70	0	0	0	0	3 (0.03%)	0.02	956 (9.46%)	0.07
Truck	0 (0.01%)	0	**5,415 (53.6%)**	1.75	0	0	0	0	-	-	**5,415 (53.6%)**	1.64
Bus	0	0	214 (2.11%)	**2.83**	-	-	0	0	0 (0.01%)	0.09	214 (2.11%)	1.89
SUV	2 (0.02%)	0.02	2,165 (21.4%)	0.63	0	0	0	0	0	0.02	2,167 (21.4%)	0.60
Van	0	0	1,127 (11.2%)	1.53	0	0	0	0	0	0.02	1,127 (11.2%)	1.20
Taxi	-	-	-	-	0	0	-	-	-	-	0	0
Special	0	0	230 (2.28%)	2.82	0	0	-	-	-	-	230 (2.28%)	**2.81**
Motorcycle	0	0	-	-	-	-	-	-	-	-	0	0
Total	146 (1.44%)	0.01	**9,959 (98.5%)**	**1.16**	0	0	0	0	3 (0.03%)	0.02	10,108 (100%)	0.41

1008

1009

1010

1011 (d) CO

Vehicle	Gasoline		Diesel		LPG		CNG		Hybrid		Total	
	Emission	IF	Emission	IF	Emission	IF	Emission	IF	Emission	IF	Emission	IF
Sedan	178,121 (47.6%)	17.1	3,436 (0.92%)	2.98	42,886 (11.5%)	23.6	29 (0.01%)	2.91	177 (0.05%)	1.07	**224,649 (60.1%)**	16.6
Truck	254 (0.07%)	61.1	47,065 (12.6%)	15.2	9,088 (2.43%)	44.9	68 (0.02%)	51.4	-	-	56,475 (15.1%)	17.1
Bus	0 (0.00%)	19.3	7,633 (2.05%)	**101**	-	-	1542 (0.41%)	41.3	1 (0.00%)	4.64	9,176 (2.45%)	**81.2**
SUV	2,616 (0.70%)	19.6	13,401 (3.58%)	3.87	791 (0.21%)	38.6	0 (0.00%)	4.09	2 (0.00%)	1.15	16,808 (4.50%)	4.65
Van	131 (0.04%)	43.4	6,611 (1.77%)	8.97	8,032 (2.15%)	40.9	2 (0.00%)	6.53	0 (0.00%)	1.00	14,777 (3.95%)	15.8
Taxi	-	-	-	-	8,481 (2.27%)	14.7	-	-	-	-	8,481 (2.27%)	14.7
Special	13 (0.00%)	269	4,224 (1.13%)	51.7	1 (0.00%)	3.69	-	-	-	-	4,239 (1.13%)	51.7
Motorcycle	39,256 (10.5%)	18.2	-		-	-	-	-	-	-	39,256 (10.5%)	18.2
Total	**220,390 (59.0%)**	17.3	82,372 (22.0%)	9.57	69,281 (18.5%)	**24.6**	1641 (0.44%)	33.6	180 (0.05%)	1.07	373,864 (100%)	15.4

1012

1013 (e) SO_x

Vehicle	Gasoline		Diesel		LPG		CNG		Hybrid		Total	
	Emission	IF	Emission	IF	Emission	IF	Emission	IF	Emission	IF	Emission	IF
Sedan	51.3 (29.8%)	0.005	6.5 (3.79%)	0.006	8.28 (4.81%)	0.005	0	0	1.14 (0.67%)	0.007	**67.2 (39.1%)**	0.005
Truck	0.03 (0.02%)	0.008	45.5 (26.5%)	0.015	0.97 (0.57%)	0.005	0	0	-	-	46.5 (27.1%)	0.014
Bus	0 (0.00%)	0.003	10.8 (6.26%)	**0.143**	-	-	0	0	0.01 (0.01%)	0.047	10.8 (6.26%)	**0.095**
SUV	0 (0.00%)	0.000	18.2 (10.6%)	0.005	0.00 (0.00%)	0.000	0	0	0.01 (0.01%)	0.007	18.2 (10.6%)	0.005
Van	0.02 (0.01%)	0.006	5.5 (3.20%)	0.007	0.77 (0.45%)	0.004	0	0	0 (0.00%)	0.010	6.30 (3.66%)	0.007
Taxi	-	-	-	-	7.71 (4.49%)	0.013	-	-	-	-	7.71 (4.48%)	0.013
Special	0 (0.00%)	0.003	7.3 (4.27%)	0.090	0.00 (0.00%)	0.005	-	-	-	-	7.34 (4.27%)	0.090
Motorcycle	7.94 (4.62%)	0.004	-		-	-	-	-	-	-	7.94 (4.62%)	0.004
Total	59.3 (34.5%)	0.006	**93.8 (54.5%)**	**0.011**	17.7 (10.3%)	0.006	0	0	1.17 (0.68%)	0.007	172 (100%)	0.007

1014

1015

1016 (e) NH_3

Vehicle	Gasoline		Diesel		LPG		CNG		Hybrid		Total	
	Emission	IF	Emission	IF	Emission	IF	Emission	IF	Emission	IF	Emission	IF
Sedan	12,225 (98.3%)	**1.17**	20 (0.16%)	0.02	0	0.00	0	0	19 (0.15%)	0.11	**12,284 (98.6%)**	**0.91**
Truck	0 (0.00%)	0.03	82 (0.66%)	0.03	0	0.00	0	0	-	-	82 (0.66%)	0.02
Bus	0 (0.00%)	0.09	15 (0.12%)	0.19	-	-	0	0	0 (0.00%)	0.51	15 (0.12%)	0.13
SUV	0 (0.00%)	0.00	0 (0.00%)	0.00	0	0.00	0	0	0 (0.00%)	0.16	0 (0.00%)	0.00
Van	0 (0.00%)	0.02	14 (0.11%)	0.02	0	0.00	0	0	0 (0.00%)	0.09	14 (0.11%)	0.01
Taxi	-	-	-	-	0	0.00	-	-	-	-	0 (0.00%)	0.00
Special	0 (0.00%)	0.01	10 (0.08%)	0.12	0	0.00	-	-	-	-	10 (0.08%)	0.12
Motorcycle	49 (0.39%)	0.02	-		-	-	-	-	-	-	49 (0.39%)	0.02
Total	**12,293 (98.7%)**	**0.97**	141 (1.13%)	0.02	0	0.00	0	0	19 (0.16%)	0.12	12,453 (100%)	0.51

1017

1018

1019 **Figures**
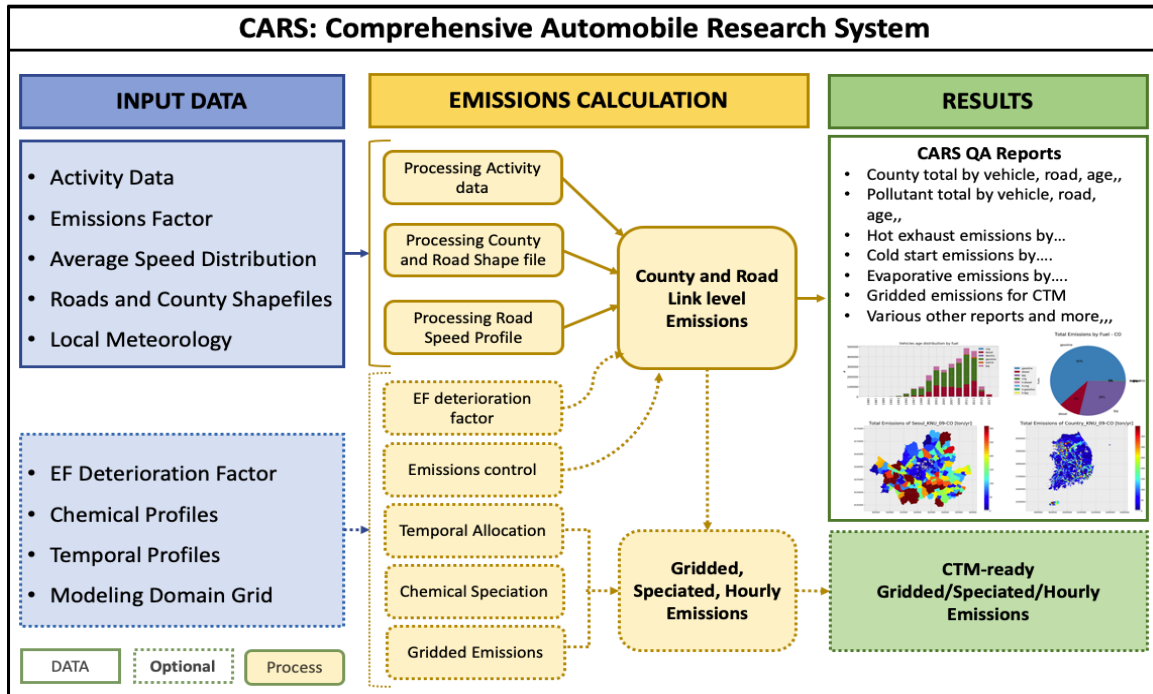
1020

1021 **Figure 1**. CARS schematic methodology to estimate mobile emissions.

1022
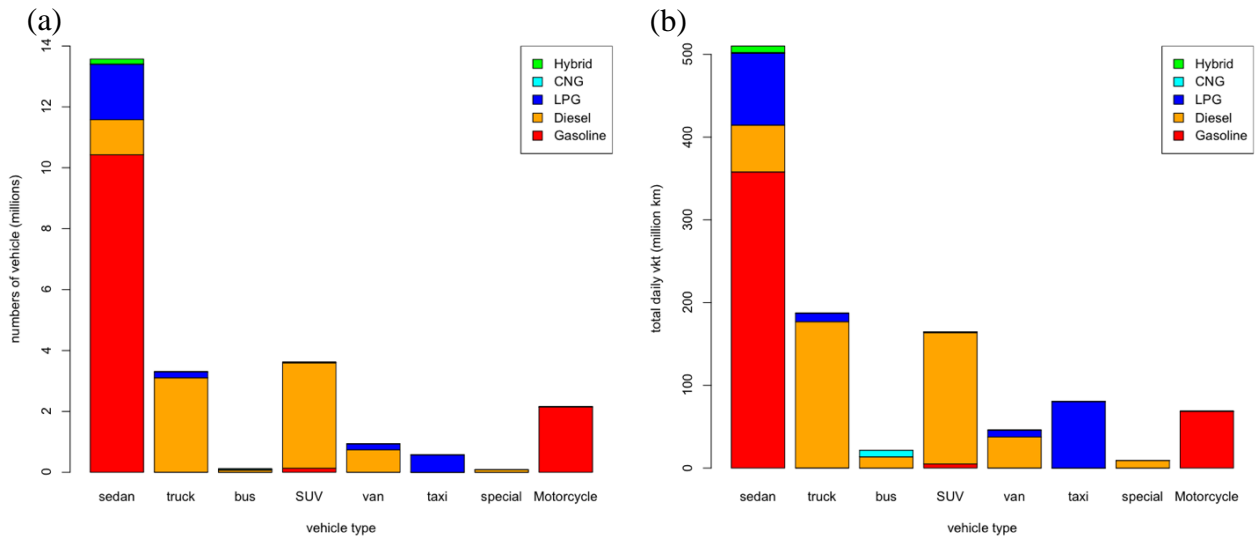
1023

1024 **Figure 2. (a)** The number of vehicles by vehicle and fuel types and **(b)** the total daily VKT by
1025 vehicle and fuel types in South Korea.

1026
1027
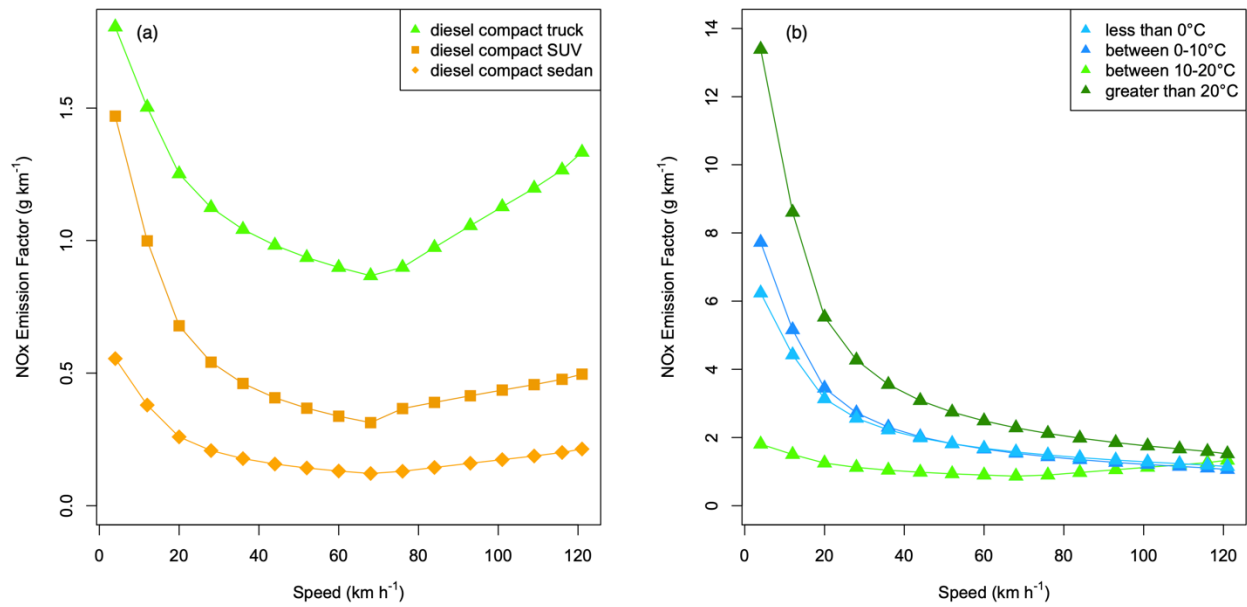
1028

1029   **Figure 3**. Variation of NOx emission factors from diesel compact engines by vehicle speed and
1030   ambient temperatures: **(a)** NO_x emission factors function to vehicle speed; **(b)** NO_x emission
1031   factors of diesel compact truck function to vehicle speed and ambient temperature.

1032
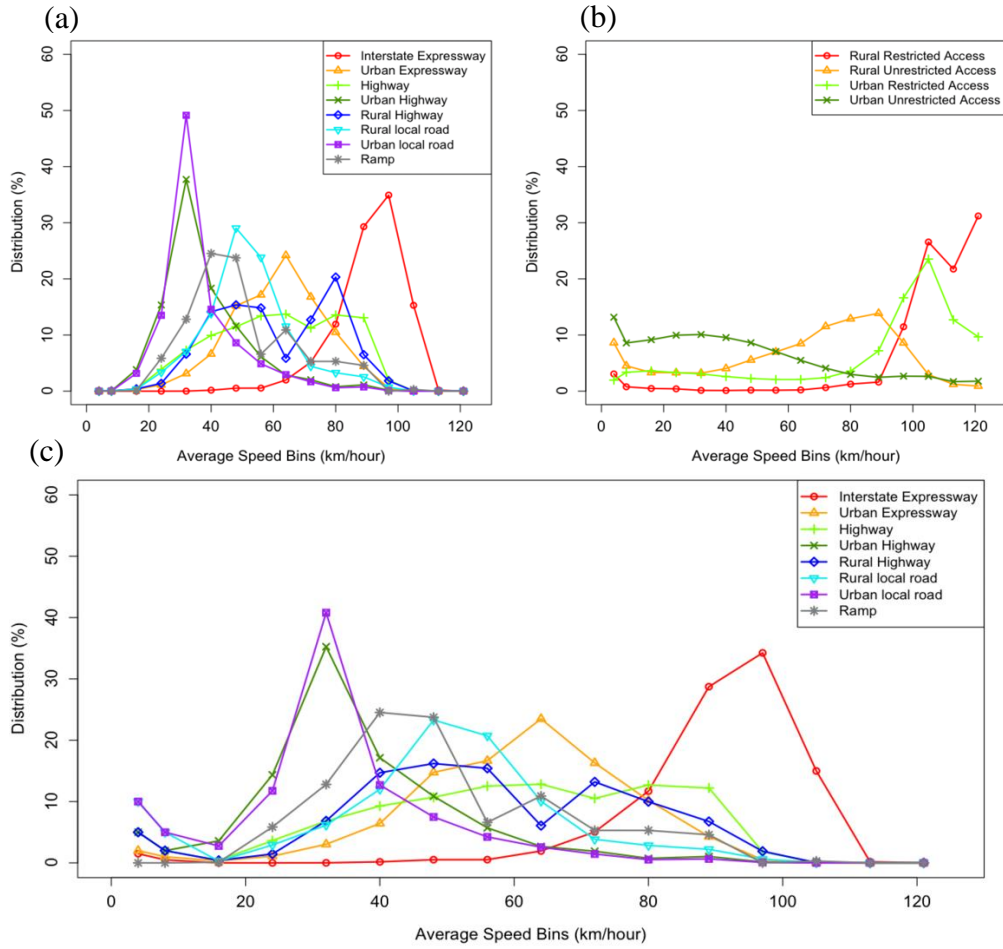
1033

1034

Figure 4. (a) The South Korea speed distribution by road types. (b) The Georgia state speed distribution by road types. (c) The average speed distribution (ASD) by road types used in this study for South Korea.

1035
1036
1037
1038
1039
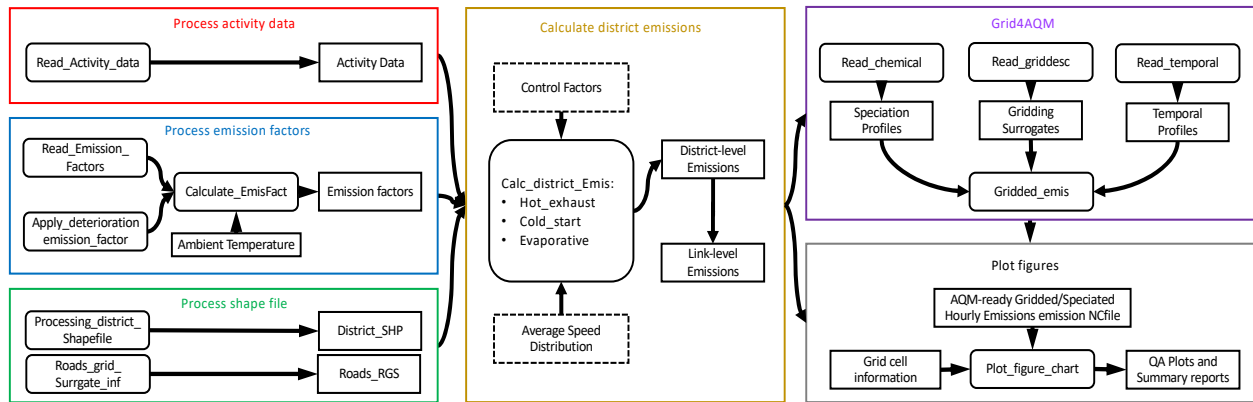
1040
1041 **Figure 5**. The schematic of modules and their functions in the CARS.
1042
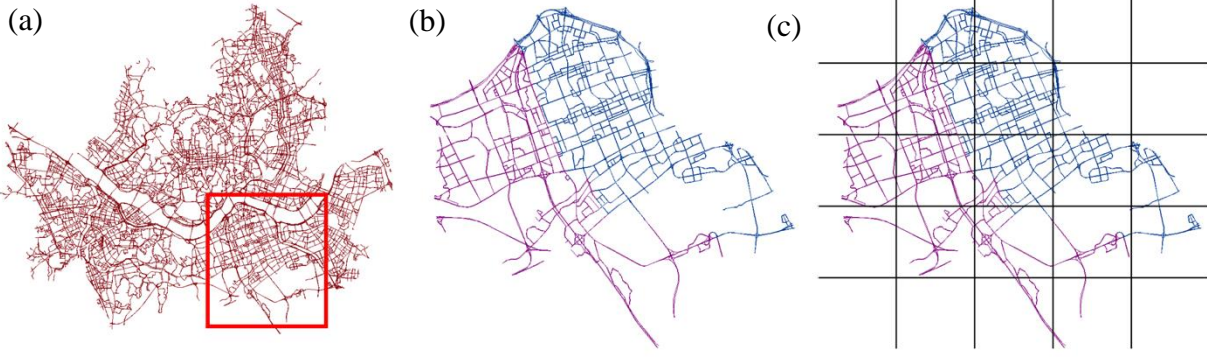
1043

1044 **Figure 6 (a)** the road network GIS shapefile of Seoul, South Korea; **(b)** two districts with different

1045 colors (purple and blue); **(c)** the modeling grid cells over road segments.

1046
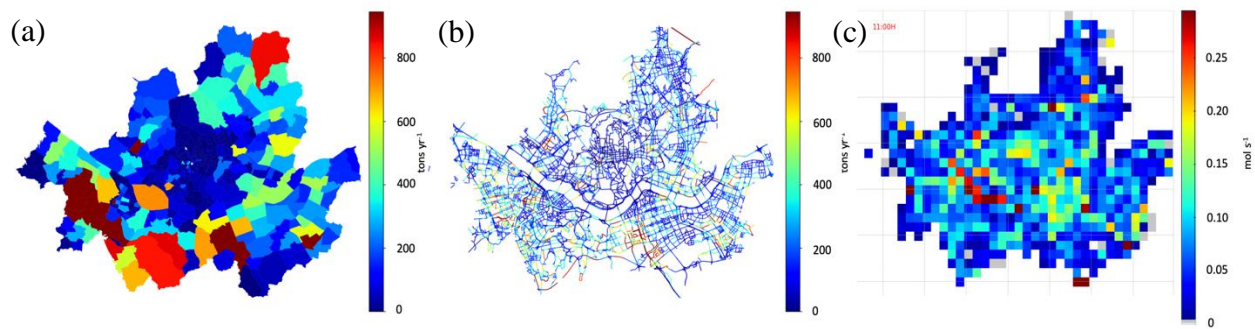
1047

Figure 7. Three different formats of CO emissions from CARS, (A) District-level total emissions
$(t\ yr^{-1})$ (B) Link-level total emissions $(t\ yr^{-1})$, (C) CTM-ready gridded hourly total emissions (moles
s^{-1}).

1051
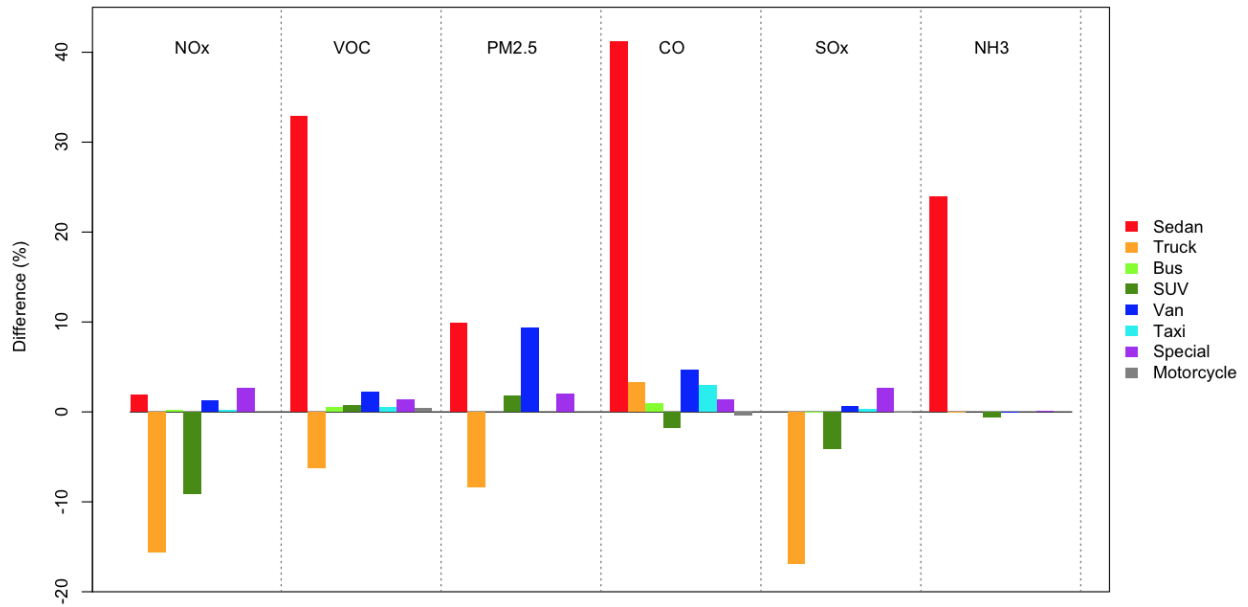
1052
1053 **Figure 8**. Comparison between CARS 2015 and CAPSS 2015 onroad mobile emissions
1054 inventories by vehicle types. The standard line is CAPSS 2015 data.
1055
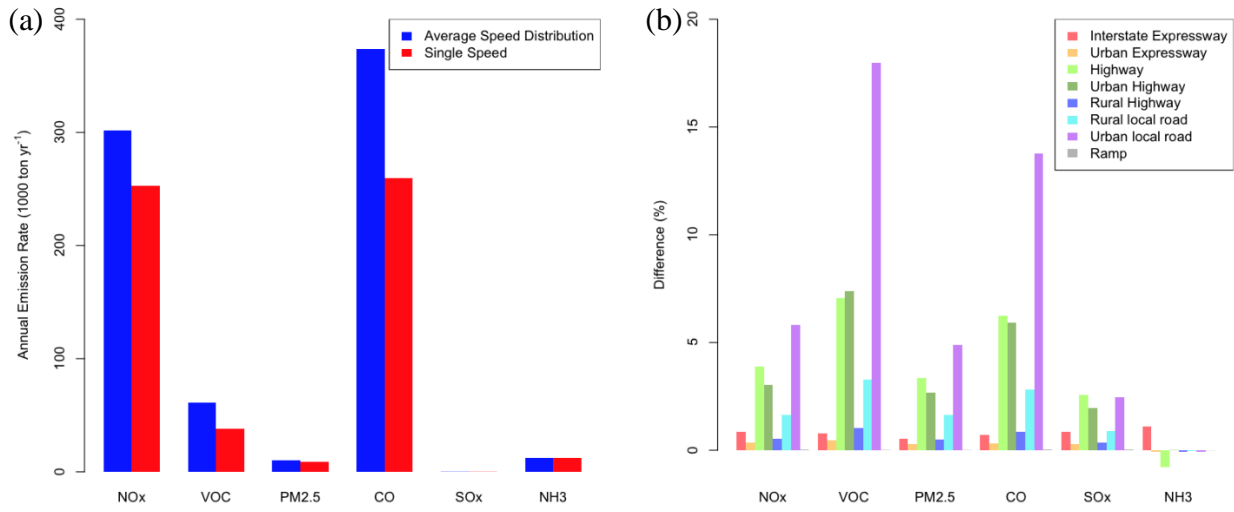
Figure 9. The impacts of emissions between the ASD and single-speed approach: (a) the total
emission differences by pollutant; (b) The road-specific difference (%) by pollutant.

1060

Appendices

Appendix A: The vehicle types classified by fuel type, vehicle body type, and engine size. The emission factors of the diesel vehicle with the star (*) are depended on the ambient temperature (*T*).

Vehicle Types	Fuel Types							
	Gasoline	Diesel	LPG	CNG	HYBRID_G	HYBRID_D	HYBRID_L	HYBRID_C
Sedan	Supercompact	Supercompact*	Supercompact	-	-	-	-	-
	Compact	compact*	compact	compact	compact	compact	compact	-
	Fullsize	Fullsize*	Fullsize	Fullsize	Fullsize	Fullsize	Fullsize	-
	Midsize	Midsize*	Midsize	Midsize	Midsize	Midsize	Midsize	-
Truck	Supercompact	Supercompact	Supercompact	-	-	-	-	-
	Compact	Compact*	Compact	Compact	-	-	-	-
	Fullsize	Concrete	-	Fullsize	-	-	-	-
	Midsize	Fullsize	Midsize	Midsize	-	-	-	-
	-	Midsize	-	-	-	-	-	-
	-	Dump	-	-	-	-	-	-
	-	Special	Special	Special	-	-	-	-
Bus	Urban	Urban	Urban	Urban	-	Urban	-	-
	-	Rural	-	Rural	-	Rural	-	Rural
SUV	Compact	Compact*	Compact	-	-	-	-	-
	Midsize	Midsize*	Midsize	Midsize	Midsize	-	-	-
Van	supercompact	supercompact	supercompact	-	-	-	-	-
	Compact	Compact	Compact	Compact	-	-	-	-
	-	-	Fullsize	Fullsize	Fullsize	Fullsize	Fullsize	Fullsize
	Midsize	Midsize	Midsize	Midsize	Midsize	Midsize	Midsize	Midsize
Taxi	-	-	Compact	-	-	-	-	-
	-	-	Fullsize	-	-	-	-	-
	-	-	Midsize	-	-	-	-	-
Special	-	Tow	-	-	-	-	-	-
	Wrecking	Wrecking	Wrecking	Wrecking	-	-	-	-
	Others	Others	Others	-	-	-	-	-
Motorcycle	Compact	-	-	-	-	-	-	-
	Midsize	-	-	-	-	-	-	-
	Fullsize	-	-	-	-	-	-	-

- no existence
* ambient temperature-dependent diesel vehicle
LPG: Liquefied Petroleum Gas
CNG: Connecticut Natural Gas
Hybrid_G: hybrid vehicle with gasoline
Hybrid_D: hybrid vehicle with diesel
Hybrid_L: hybrid vehicle with LPG
Hybrid_C: hybrid vehicle with CNG

Appendix B, The summary of activity data (number of vehicles and daily total VKTs) in South
Korea by vehicle type with engine size.

Vehicle Types	Engine sizes	Fuel Types									
		Gasoline		Diesel		LPG		CNG		Hybrid	
		Numbers	Daily VKT	Numbers	Daily VKT	Numbers	Daily VKT	Numbers	Daily VKT	Numbers	Daily VKT
Sedan	Supercompact	1,792,471	50,197,345	46	1,761	83,226	4,000,067	6	237	-	-
	Compact	1,372,317	39,543,668	51,324	2,570,086	8,040	257,060	276	12,115	3,802	137,360
	Fullsize	2,403,327	100,632,702	428,831	20,928,552	292,850	15,910,588	5,296	323,852	21,533	1,086,509
	Midsize	4,858,533	167,454,032	672,960	33,126,318	1,431,970	66,640,378	4,310	625,717	140,527	6,717,856
Truck	Supercompact	850	9,595	816	354	111,051	6,550,476	-	-	-	-
	Compact	3,185	143,510	2,655,089	133,480,216	87,650	3,567,109	42	2,694	-	-
	Fullsize	3	422	180,991	25,774,819	-	-	72	4,676	-	-
	Midsize	98	7,430	258,509	17,477,685	1,434	47,870	14	483	-	-
	Dump	-	-	-	-	-	-	-	-	-	-
	Special	20	970	-	-	2,292	99,124	1,194	60,886	-	-
Bus	Urban	1	126	40,448	7,282,593	1	652	6,543	1,466,854	2	282
	Rural	-	-	34,997	6,334,278	-	-	30,792	6,460,001	216	50,873
SUV	Compact	42,348	1,395,153	2,341,397	105,962,626	6,946	275,728	13	551	-	-
	Midsize	91,002	3,520,552	1,120,128	5,277,861	13,567	595,426	15	706	1,719	88,683
Van	supercompact	88	1,645	-	-	44,947	2,058,014	-	-	-	-
	Compact	2,937	87,507	685,317	34,781,937	151,654	6,135,138	7	255	-	-
	Fullsize	-	-	19,452	1,318,221	1	14	97	7,598	3	136
	Midsize	2	1,303,795	31,790	1,433,407	15	416	160	15,216	2	85
	Special	-				-				-	
Taxi	Compact	-	-	-	-	8,380	576,378	-	-	-	-
	Fullsize	-	-	-	-	92,861	10,827,756	-	-	-	-
	Midsize	-	-	-	-	474,455	69,087,721	-	-	-	-
Special	Tow	-	-	40,807	7,447,773	-	-	-	-	-	-
	Wrecking	2	138	12,568	813,746	128	6,607	3	94	-	-
	Others	47	553	28,275	989,988	180	9,966	-	-	-	-
Motorcycle	Compact	184,822	3,507,948	-	-	-	-	-	-	-	-
	Fullsize	65,964	3,493,728	-	-	-	-	-	-	-	-
	Midsize	1,910,988	61,676,824	-	-	-	-	-	-	-	-

1079   - no existence
1080   LPG: Liquefied Petroleum Gas
1081   CNG: Connecticut Natural Gas
1082   Hybrid: all hybrid vehicles, electric power mixed with fossil fuel (gasoline, diesel, LPG, or CNG)

1083

1084

1085

1086

1087 **Appendix C**, Eight road types with assigned average vehicle operating speed and VKT fractions.

Road types	Description	Average Speed (km h^{-1})	Road VKT fraction
101	Interstate Expressway	90	41%
102	Urban Expressway	60	5%
103	Highway	58	18%
104	Urban Highway	36	12%
105	Rural Highway	55	3%
106	Rural Local Road	45	4%
107	Urban Local Road	32	17%
108	Ramp	50	0.4%

1088
1089

1090 **Appendix D,** The daily average VKT (km d^{-1}) per vehicle by vehicle and fuel types.

Vehicle types	Fuel Types					
	Gasoline	Diesel	LPG	CNG	Hybrid	Average
Sedan	34	49	48	97	48	38
Truck	39	57	51	52	-	57
Bus	126	180	-	212	237	191
SUV	37	46	42	45	52	46
VAN	29	51	42	87	44	49
Taxi	-	-	140	-	-	140
Special	14	113	54	31	-	113
Motorcycle	32	-	-	-	-	32

1091

1092

Appendix E, Average speed distribution (ASD) for each road type: The table columns are different road types, and the table rows are average speed of each speed bin.

Speed bins	Speed (km/h)	Road Types							
		101	102	103	104	105	106	107	108
1	speed < 4	1.50%	2.00%	5.00%	5.00%	5.00%	10.00%	10.00%	0.00%
2	4 ≤ speed < 8	0.50%	1.00%	2.00%	2.00%	2.00%	5.00%	5.00%	0.00%
3	8 ≤ speed < 16	0.00%	0.33%	0.40%	3.59%	0.41%	0.30%	2.76%	0.11%
4	16 ≤ speed < 24	0.00%	1.09%	3.64%	14.35%	1.45%	2.91%	11.75%	5.85%
5	24 ≤ speed < 32	0.01%	3.04%	6.82%	35.25%	6.85%	6.15%	40.80%	12.80%
6	32 ≤ speed < 40	0.17%	6.43%	9.28%	17.14%	14.70%	12.00%	12.69%	24.53%
7	40 ≤ speed < 48	0.52%	14.76%	10.70%	10.86%	16.20%	23.30%	7.49%	23.74%
8	48 ≤ speed < 56	0.53%	16.66%	12.52%	5.72%	15.42%	20.72%	4.24%	6.60%
9	56 ≤ speed < 64	1.94%	23.49%	12.83%	2.68%	6.08%	10.06%	2.56%	10.90%
10	64 ≤ speed < 72	5.05%	16.30%	10.51%	1.90%	13.21%	3.84%	1.45%	5.30%
11	72 ≤ speed < 80	11.70%	10.19%	12.69%	0.74%	9.98%	2.85%	0.53%	5.30%
12	80 ≤ speed < 89	28.73%	4.30%	12.21%	1.04%	6.75%	2.21%	0.65%	4.59%
13	89 ≤ speed < 97	34.24%	0.51%	1.82%	0.15%	1.90%	0.62%	0.08%	0.00%
14	97 ≤ speed < 105	14.99%	0.00%	0.02%	0.00%	0.04%	0.03%	0.00%	0.30%
15	105 ≤ speed < 113	0.18%	0.00%	0.00%	0.00%	0.00%	0.00%	0.00%	0.00%
16	113 ≤ speed < 121	0.01%	0.00%	0.00%	0.00%	0.00%	0.00%	0.00%	0.00%

Appendix F: Single average speed for each road type

Speed bins	Speed (km/h)	Road Types							
		101	102	103	104	105	106	107	108
1	speed < 4	0%	0%	0%	0%	0%	0%	0%	0%
2	4 ≤ speed < 8	0%	0%	0%	0%	0%	0%	0%	0%
3	8 ≤ speed < 16	0%	0%	0%	0%	0%	0%	0%	0%
4	16 ≤ speed < 24	0%	0%	0%	0%	0%	0%	0%	0%
5	24 ≤ speed < 32	0%	0%	0%	0%	0%	0%	100%	0%
6	32 ≤ speed < 40	0%	0%	0%	100%	0%	0%	0%	0%
7	40 ≤ speed < 48	0%	0%	0%	0%	0%	100%	0%	100%
8	48 ≤ speed < 56	0%	0%	100%	0%	100%	0%	0%	0%
9	56 ≤ speed < 64	0%	100%	0%	0%	0%	0%	0%	0%
10	64 ≤ speed < 72	0%	0%	0%	0%	0%	0%	0%	0%
11	72 ≤ speed < 80	0%	0%	0%	0%	0%	0%	0%	0%
12	80 ≤ speed < 89	100%	0%	0%	0%	0%	0%	0%	0%
13	89 ≤ speed < 97	0%	0%	0%	0%	0%	0%	0%	0%
14	97 ≤ speed < 105	0%	0%	0%	0%	0%	0%	0%	0%
15	105 ≤ speed < 113	0%	0%	0%	0%	0%	0%	0%	0%
16	113 ≤ speed < 121	0%	0%	0%	0%	0%	0%	0%	0%

 Appendix G:

 The annual emission rate between original road type ASD, adjusted road type ASD, and CAPSS
 result for 2015

Gg/year	CO	NOx	SOx	PM10	PM2.5	VOC	NH3
CARS data 2015 org ASD	269.3	258.4	0.2	9.5	8.8	38.9	12.4
CARS data 2015 adj ASD	373.9	301.8	0.2	11.0	10.1	61.2	12.5
CAPSS 2015	245.5	369.6	0.2	9.6	8.8	46.1	10.1

 Appendix H:

 CARS model input data summary table

Input data type	Parameters	Variable Name in CARS	File format
Human activity data of each vehicle	Fuel, vehicle, type, daily VKT, region code, manufacture data	activity_file	csv
Emission factor table	Vehicle, engine, fuel, SCC ,Pollutant, year, temperature, v,a,b,c,d,f,k	Emis_factor_list	csv
Link level Shape file	Link ID, region code, region name, road rank, speed, VKT, Link length, geometry	Link_shape	shape file
County Shape File	Region code, region name	county_shape	shape file
Average speed distribution table	Speed bins, the distribution of each road type	avg_SPD_Dist_file	csv
road restriction table	Vehicle, engine, fuel, road types	road_restriction	csv
Vehicle deterioration table	Vehicle, engine, SCC, fuel, Pollutant, Manufacture date	Deterioration_list	csv
Control strategy factors table	Vehicle, engine, fuel, year, data, region code, control factor	control_list	csv
Model domain description	Projection method name, parameters for prjection method, domain name, bottum left coner X and Y, grid cell size, numbers of grid cell in X, Y, and Z-axis	gridfile_name	text file in griddesc format
Temporal profile tables	Profile reference number, Year to Monthly profile (12 columns)	temporal _monthly_file	csv
	Profile reference number, week to daily profile (7 columns)	temporal _week_file	csv

	Profile reference number, week day to hourly profile (24 columns)	temporal_weekday_file	csv
	Profile reference number, weekend day to hourly profile (24 columns)	temporal_weekend_file	csv
	Vehicle, types, fuel, road type, month reference number, week reference number, weekday reference number, weekend reference number	temporal_CrossRef	csv
Chemical profile table	Species code, species name, target species name, fraction, molecular weight,	Chemical_profile	txt or csv
	Vehicle, engine, fuel, species reference codes	speciation_CrossRef	csv

1107
1108